9-22-2020

Investigation of the sequence-structure-activity relationship in Ponericin L1 from Neoponera Goeldii & synergistic interactions of ionic liquids and antimicrobials to improve efficacy

Alexandria S. Senetra
Rowan University

INVESTIGATION OF THE SEQUENCE-STRUCTURE-ACTIVITY RELATIONSHIP IN PONERICIN L1 FROM *NEOPONERA GOELDII* & SYNERGISTIC INTERACTIONS OF IONIC LIQUIDS AND ANTIMICROBIALS TO IMPROVE EFFICACY

by

Alexandria S. Senetra

A Thesis

Submitted to the
Department of Chemistry and Biochemistry
College of Science and Mathematics
In partial fulfillment of the requirement
For the degree of
Master of Science in Pharmaceutical Sciences
at
Rowan University
July 23, 2020

Thesis Chair: Gregory A. Caputo, Ph.D.

Dedication

This thesis is dedicated to my mom Stephanie, who has raised me to be the person I am today. You have been with me every step of the way, even when facing challenges and obstacles. Thank you for your unconditional love, support, and guidance you have given me. You have helped me succeed in life, instilling the confidence I need to understand that I am capable of doing anything I put my mind to. I appreciate all that you have done for me to help me throughout this difficult journey. This girl is on fire.

Acknowledgments

First and foremost, I would like to express the deepest appreciation to my thesis advisor, Dr. Caputo. His expertise, consistent guidance, dedication, and persistent advice helped me through my undergraduate and graduate education preparing me for my doctorate. I had never imagined pursuing a master's degree, let alone being able to get into a doctorate program. Throughout all my challenges and setbacks, he always encouraged me to keep going. Dr. Caputo helped mold me into the best I could be, and pushed me farther than I thought I could go.

My appreciation also extends to my laboratory colleagues throughout the five years I was a part of Dr. Caputo's lab. Thank you for always helping me out when I needed it, and making my time at Rowan memorable.

Finally, I must express my gratitude to my family and friends for providing me with unfailing support and continuous encouragement throughout my educational journey. They have helped me understand the value of dedication to achieve my goals and what it means to have a great team cheering you on. This accomplishment would not have been possible without any of these people. Thank you for your unwavering support.

Abstract

Alexandria S. Senetra
INVESTIGATION OF THE SEQUENCE-STRUCTURE-ACTIVITY RELATIONSHIP IN PONERICIN L1 FROM *NEOPONERA GOELDII*
&
SYNERGISTIC INTERACTIONS OF IONIC LIQUIDS AND ANTIMICROBIALS TO IMPROVE EFFICACY
2019-2020
Gregory A. Caputo, Ph.D.
Master of Science in Pharmaceutical Sciences

Non-traditional antimicrobials have been an area of great interest due to the increasing prevalence of antimicrobial resistance (AMR) in bacteria. Antimicrobial peptides (AMPs) & ionic liquids (ILs) are two examples that have been investigated as a potential solution. Most AMPs are naturally derived & exhibit high selectivity against bacterial targets over host cells. The venom-derived peptide, ponericin L1 from *Neoponera goeldii,* was used to investigate the role of cationic residues & net charge on peptide activity. Using both in vitro & microbiological methods, L1 peptide & derivatives exhibited an α-helical conformation with enhanced binding to lipid vesicles containing anionic lipids & low hemolytic activity. Net charge & identity of the cationic groups on the peptide were shown to play a significant role in antimicrobial activity. ILs have also been investigated in combination with antimicrobial compounds to fight AMR. Imidazolium chloride-based ILs with differing alkyl tails & commercially available antibiotics were used to examine the potential for synergistic effects on multiple bacteria. Analysis of the IL data indicates that length of the alkyl chain play a crucial role in antimicrobial activity & cytotoxicity. A synergistic effect was exhibited while showing low cytotoxicity when tested in a mammalian cell culture model.

Table of Contents

Table of Contents (Continued)

Table of Contents (Continued)

List of Figures

List of Tables

Chapter 1

Overview of Antimicrobials

Background

History of antimicrobials. For thousands of years, infections had reached epidemic proportions costing the lives of millions [1]. There have been many interventions throughout time to prevent and control the spread of infection. For example, in 1846, a Hungarian physician, Semmelweis, found that mortality from childbed fever in women who delivered babies by midwives was lower than those delivered by physicians. Semmelweis concluded that this issue was a result of cadaverous materials on the hands of medical students who came from the autopsy chamber to the obstetric clinic. This led to the implementation of hand washing in a chlorinated lime solution before having contact with patients, dropping the mortality rate among women that were being cared for by physicians [2]. Another groundbreaking discovery occurred in 1928, when Alexander Fleming found the first antibiotic, penicillin [3-4]. Then, the discovery that bacteria could be isolated, cultured and act as a bioactive molecule was identified. In 1941, the term *antibiotic* was first used by Selman Waksman to describe any small molecule produced by a microbe that prevents the growth of another microbe [5]. Multiple antibiotic classes with different targets were discovered and soon an assembly line production of penicillin, streptomycin, chloramphenicol, and tetracycline were the segue to the antibiotic age (1945-1955).

Discovery, commercialization, and routine administration of antibiotics has become one of the most important medical interventions to treat infectious diseases [6].

Millions of lives have been saved due to antibiotics [7]. Although, antibiotics are known to save lives, the over-prescribing have arguably led to the epidemic of multi-drug resistant (MDR) microbes [8]. The capability for multiple types of bacteria to rapidly develop mechanisms of resistance to common medications threatens the prevention and treatment for infections. Antimicrobial resistance (AMR) has become a major health threat globally due to an increased mortality rate in people with a multi-drug resistant bacterial infection [9].

When treating a multi-drug resistant (MDR) infection, even some of the most potent antibiotics are unable to kill these "superbugs" [4]. With delayed development of new antibiotics [10], there is an urgent need for novel antimicrobial strategies and/or alternative drugs to revive the potency of traditional antibiotics, prevent mortality, and help reduce the chances of antimicrobial resistance [11]. An example of a new antimicrobial drug is antimicrobial peptides (AMPs). AMPs are a growing class of naturally derived novel antibacterial molecules with unique antimicrobial mechanisms. In various organisms such as plants, animals, and humans, AMPs contain important components for the innate immune system, which become the first-line defense against an infection [12-13].

History of antimicrobial peptides. In 1939, Dubos isolated tyrothricin, an antimicrobial agent, from a spore-bearing soil *Bacillus* strain, which protected mice from a pneumococci infection [14]. This led to the first discovery of an AMP named gramicidin [15]. Although toxicity was associated with intraperitoneal application, gramicidin was effective in treating wounds and ulcers topically [16]. Another AMP extracted from tyrothricin, tyrocidine, was discovered in 1941, and exhibited

antimicrobial activity against both Gram-negative and Gram-positive bacteria [17]. Although tyrocidine was effective against bacteria, strong hemolytic activity was also shown, making it a poor choice for a therapeutic [18]. Later that year, purothionin was isolated from the plant *Triticumaestivum* and was effective against some pathogenic bacteria, along with fungi [19]. In 1956, the first animal isolated AMP was a defensin found in rabbit leukocytes [20]. Defensins are the largest class of mammalian AMPs and have been found throughout evolution. They play a key role in the innate immune response to infection, as well as being implicated in wound healing and immune modulation [180].

As of 2016, there have been over 23,000 AMPs discovered including both natural and synthetic [21]. Natural AMPs have been found in various sources such as bacteria, invertebrates, vertebrates, and plants [22]. AMPs extracted from animals are mainly found in the tissues and organs exposed to airborne pathogens to stop most infections before symptoms develop [23], [24]. There are various types of eukaryotic cells involved in the production of AMPs including epithelial cells in gastrointestinal and genitourinary systems [25-26], phagocytes [27], and lymphocytes of the immune system [28-29]. Frog skin, for example, contains over 300 different AMPs [30-31]. An example of an AMP extracted from the ventral skin of the frog, *Xenopus laevis,* is called magainin [32]. Magainins are produced by the mucous glands in the skin of the frog and exhibit broad-spectrum antimicrobial activity against bacteria, fungi, and protozoa [33].

Structures and characteristics of antimicrobial peptides. AMPs are normally amphipathic, cationic peptides with a varying amino acid chain of about five to less than 50 exhibiting an overall positive charge. AMPs have shown interaction with a broad

spectrum of organisms, such as bacteria, including multi-drug resistant bacteria [34], cancer [35], viruses [36], fungi [37], and even parasites [38]. They have also been shown to rapidly kill cells in seconds after initial contact with their target [39].

Based on their secondary structure, AMPs are characterized as α-helix, β-sheet, extended, and loop, with α-helix and β-sheet AMPs being the most common [40]. The α-helical peptides are cationic and amphipathic with some level of hydrophobicity that possess antimicrobial activity [41]. Some α-helical AMPs are rich in the amino acids, His and Trp. Examples of α-helical AMPs are protegrin, magainin, and LL37 (a human cathelicidin) [42]. AMPs classified under β-sheet contain at least two β-strands with disulfide bonds between the strands [43]. Although most AMPs belong to one of the four categories listed above, some do not belong to any of them [44], and can contain two different structural components [45]. Among the four categories of AMPs, the α-helical AMPs are one of the most studied types [46].

Mechanism of action of antimicrobial peptides. Most peptides only form their active structure once they are interacting with their target membranes. Commercially-available antibiotics target specific cellular activities, while AMPs are proposed to use a multitude of complementary actions to cause cell death [47]. AMPs kill target cells by disrupting the membrane integrity by inhibiting proteins, DNA and RNA synthesis, or by interacting with specific intracellular targets. Due to their multi-hit mechanism, this reduces the possibility of bacterial drug resistance in AMPs ultimately increasing the efficiency of AMPs [48].

AMPs initial interaction with the bacterial cell membrane occurs through electrostatic bonding between the positively charged peptide and negatively charged components located on the outer bacterial envelope [49]. Since AMPs are composed of cationic and hydrophobic residues, there is a strong interaction with a bacterial membrane that contains negatively charged lipids such as phosphatidylglycerol or cardiolipin [50]. The most common explanation of AMPs selectivity for bacterial cells over host cells are the difference in membrane interactions caused by the exposed anionic lipid content present in bacterial membranes [3]. Since electrostatic interactions play a key role in the binding of AMPs to bacterial membranes, the interactions with the neutral phosphatidylcholine/cholesterol-rich surfaces of prokaryotic membranes are significantly weaker.

Although the mechanism of action for AMPs are not fully understood, there are many proposed pathways to disrupt the bacterial cell membrane that AMPs use. A few models include the barrel-stave pore, the toroidal pore, and the carpet model [51]. In the barrel-stave pore model, peptides are shown interacting laterally with one another to form a structure similar to a membrane protein ion channel, while in the toroidal pore model peptide-peptide interactions are not present. Instead, the peptides induce a curvature of the bilayer to create a high curvature form. The major difference between these two models are that the barrel-stave pores are working with the bilayer hydrocarbon core, ultimately using it as a template for peptide-self-assembly, while the toroidal pores are working against the core, disrupting the segregation of the polar and non-polar parts, to provide a surface where lipid hydrocarbons and headgroups are able to interact favorably [50]. The carpet model was proposed in 1996 by Shai to explain the mechanism of action

of a mammalian cecropin P1 on model membranes. Their proposed model consists of the peptide micelle coating a small area of the membrane surface where AMP molecules penetrate the lipid bilayer, letting pore formation occur [52]. This method leaves behind holes or pores in the membrane [53]. The AMP is only active when aggregation of peptides align (to form a carpet-like structure) with the lipid bilayer [54].

Physiochemical properties of antimicrobial peptides. Since AMPs are composed of amino acids, modification to their sequence is relatively easy to perform, which helps to modify activity and target spectrum, along with improving stability of AMPs [55-56]. Important physiochemical properties of AMPs for their antimicrobial activity and target specificity include size, net charge, hydrophobicity, amphipathicity, and solubility [46]. Length is an important factor in AMPs because when forming an amphipathic structure with hydrophobic and hydrophilic faces on opposite sides, at least 7-8 amino acids are needed. Although length effects its 3D structure and potential mode of action, it may also affect its cytotoxicity [57]. A study showing a shortened melittin with 15 residues at its C-terminal exhibited at least 300 times less toxicity to rat erythrocytes, compared to its original form [58]. In another study, a derivative of HP-A3, with deletion of the N-Terminal random coil (residues 2-5; called A3-NT) exhibited higher antimicrobial activity with no hemolytic activity even at high concentrations of peptide [59]. These examples show length should be considered while designing a low toxicity synthetic peptide.

The sum of all charges of ionizable groups of the peptide is known as the net charge. The charge can vary from negative to positive but is the main factor for initial interaction between negatively charged bacterial cell membranes. Most α-helical cationic AMPs

contain at least a net positive charge of at least +2 [181]. Many studies have shown net charge can affect the AMPs hemolytic and antimicrobial activities, to selectively kill microbes with minimal effects on the host cells [4]. For example, a study performed by Dathe *et al.* showed that an increase in net charge of magainin 2 from +4 to +5 increased antimicrobial activity. However, an increase to +7 did not increase the observed antimicrobial activity but did increase hemolytic activity [182].

Hydrophobicity has also shown influences the activity and selectivity of AMPs. Natural AMPs contain about 50% hydrophobic residues in its sequence. It has been shown that when the hydrophobicity increases on the positively charged side of an AMP below a threshold can increase its antimicrobial activity, and when hydrophobicity is decreased it reduces the antimicrobial activity [42, 60]. There have also been studies showing that hydrophobic residues play an important role in hemolytic activity [183]. For example, a study performed by Chang *et al.*showed peptides containing hydrophobic residues of N-terminal hydrophobic core were involved in the hemolytic and bactericidal activity. When they increased the hydrophobicity in the peptides tested, both bactericidal and hemolytic activity was reduced. AMPs do have an optimal window of hydrophobicity, and once passed it has a rapid decrease in activity [61].

Another important property of AMPs is amphipathicity. This helps ensure activity and interaction with bacterial cell membranes. A study performed by Fernandes-Vidal *et al.* had shown amphipathicity helps create a strong partition for the AMP to get into the membrane interface [62]. This makes amphipathicity more important than hydrophobicity when binding to bacterial cell membranes.

AMPs solubility in aqueous environments are essential due to initial interactions with the bacterial membrane. If the AMP molecules aggregate, it will lose its ability to interact with the bacterial cell membrane, making solubility an important factor. Each of these properties, length, net charge, hydrophobicity, helicity, amphipathicity, and solubility should be taken into consideration when designing a novel peptide. AMPs have evolved to balance each of these properties to maintain optimal function.

Modifications to antimicrobial peptides. There are many factors that affect the activity of AMPs. It has been shown that modification of an AMPs properties can alter other properties. Even a small change in the primary sequence has been shown to affect physiochemical properties necessary for the activity of an AMP to interact with its target cell [46]. Although many AMPs are directly synthesized in their active forms, some AMPs require post-translational modification to perform their intended functions.

Venom-derived antimicrobial peptides. A particular category of AMPs that have been studied and modified, are venom-derived peptides. Venoms contain a mixture of peptides, proteins, and enzymes serving as either predation and defense against microbes and predators [63]. Although there are many venom-derived peptides that have antimicrobial activity, not all peptides are AMPs or even biologically active when extracted. Venoms are comprised of a diverse array of different biologically active peptides with a myriad of activities and targets including neurotoxins, membrane permeabilizing agents, and GPCR agonists and antagonists [64-65]. In fact, venom peptides appear to have evolved from a somewhat small number of structural frameworks that are well suited to addressing the crucial issues of potency and stability [65]. These bioactive peptides are small in size, relatively easy to synthesize in the lab, and have

significant structural stability and target specificity making them a novel antimicrobial component [66].

To survive chemical degradation in solution at ambient temperature and enzymatic degradation by processing proteases present in venom, these venom-derived peptides must be sufficiently stable [67]. Post-translational modifications (PTMs) and/or disulfide bonds is how these peptides are able to achieve this type of stability. Common PTMs include amidation (C-terminal), sulfation (Tyr), bromination (Trp), glycosylation (Thr), γ-carboxylation (Glu), hydroxylation (Pro), pyroglutamation, N-C-cyclization, and isomerization to D-amino acids [65]. These modifications introduce specific enzymes at particular locations during the production of venom peptides, which can help enhance bioavailability and potency along with stability. Although many of these modifications help enhance peptide properties, they are not always optimal for the requirements associated with potential therapeutic applications. Issues such as formulation, cost of production, stability, selectivity, and mechanism of action are associated with using venom peptides as therapeutics.

A significant issue with venom peptides is their bioavailability, which is generally poor due to their size (10-40 amino acids) and hydrophilic nature [65]. This issue makes it necessary for the peptide to be administered to the site of action by injection (intravenous, intrathecal, intraperitoneal, intramuscular, subcutaneous, or epidural). There have been many emerging approaches, such as lipophilic modifications, to improve peptide delivery to help eventually allow oral delivery to central and peripheral target [68]. Venom-derived peptides overall have beneficial properties such as stability, and

target specificity which are useful in antimicrobial use. However, issues including safety, pharmacokinetics, and delivery would need to be addressed before therapeutic use.

Background of ionic liquids. In addition to discovering new antimicrobials, there have been also studies performed to enhance antimicrobial efficacy with commercially available antibiotics in combination with other molecules. An example of a widely used combinatorial formulation is amoxicillin with clavulanic acid [69]. The amoxicillin is used to inhibit peptidoglycan synthesis while clavulanic acid inhibits the β-lactamase enzyme which degrades amoxicillin. Other approaches take two molecules that independently exhibit antimicrobial activity and combine the dose for treatment [70-71]. The majority of combination therapies are designed to act via different mechanisms, ultimately enhancing the activity of the other. Unfortunately, no clear best practice using these therapies have emerged, only case-specific protocols.

Ionic liquids (ILs) are a class of salts that exist in liquid form at room temperature [72-73]. ILs contain a cation and anion pair which can be changed, creating a wide range of IL species. Chemical properties of ILs include low melting point, negligible vapor pressure, and exceptional solvation potential. ILs have received attention as a potential biomaterial that can undergo modification (via changing their cations and anions) for various biomedical applications [74-75]. Other applications of ILs include use in pharmaceutics and medicine [76], and the extraction and separation of biomolecules [77]. Studies have also shown ILs ability to both stabilize and destabilize protein structures, exhibit sensitive protein interactions, enhance enzymatic activity, and impact DNA structure [78-80]. However, literature indicates that not all ILs behave similarly and that

the effects on biomolecules are dependent on the molecular identity of the components of the ILs.

Ionic liquids as antimicrobials. The interactions between ILs in aqueous solution and lipid bilayer membranes have helped guide the development of IL-based drug formulation and drug-delivery applications [76, 81-84]. Ultimately opening research avenues for IL-based antibiotics and antibiotic-IL combinatorial therapies. There have also been reports highlighting both experimental and computational studies on how ILs interact with lipid bilayers [85-86]. Hydrophobic ILs are able to insert themselves into lipid bilayers, leading to bilayer reorganization [87-89]. ILs have also exhibited antimicrobial effects with addition of enzyme-hydrolyzing groups, alkyl chains, and stable anions [90]. Additionally, a tetracycline-based IL has been shown to insert into liposome membranes with important drug-delivery and antibiotic implications [83]. The highly recombinant nature of ILs makes amenable to formulating "designer" reagents to treat specific cell types: rearranging both the anion and cation a can allow for highly specific, tailored applications in different organisms [82]. Previous studies demonstrated that IL with imidazolium-based cations were successful in permeating the membranes of bacteria, yeast, and red blood cells [91]. Other ILs have been shown to exhibit antimicrobial activity alone, or impact the manner in which antimicrobials interact with lipid bilayers [92]. Additionally, micelle formation can occur in these molecules through the interactions of the IL alkyl chains, which can influence the interactions with cellular membranes [93].

Chapter 2

Investigation of the Sequence-Structure-Activity Relationship in Ponericin L1 from *Neoponera goeldii*

Introduction

There are three categories of insect AMPs; Cecropins, Defensins, and peptides with an overrepresentation of Proline and/or Glycine residues [94]. They are separated based on their amino acid sequence and structure. Cecropins are linear peptides that lack cysteine residues but form an α-helix structure. Defensins consist of 6-8 conserved cysteine residues, are stabilized by 3 or 4 disulfide bridges and contain 3 domains that have a flexible amino-terminal loop. Cecropins are shown to exhibit antimicrobial activity against both Gram-positive and Gram-negative bacteria, while Defensins selectively kill Gram-positive, and glycine-rich and proline-rich kill Gram-negative strains [95]. Insect AMPs are considered very potent due to their IC_{50} range being in the submicromolar or even low micromolar range, even though there are none yet on the market [96]. Ponericins have been known to be one of the most explored insect AMPs, along with cecropins, drosocin, attacins, diptericins, defensins, drosomycin, and metchnikowin [97-98].

Background on ponericins. Ponericins are AMPs that were isolated from the venom of the predatory ant *Neoponera goeldii* (previously misclassified as *Pachycondyla goeldii*). There are fifteen novel ponericins extracted that exhibit both antibacterial and insecticidal properties [99]. Ponericins are classified as either G, W, and L based on their primary structure. All three classes are cationic, amphiphilic peptide sequences, with nearly all (12/15) containing a Trp residue in the N-terminal

region. Ponericins share high sequence similarities with known peptides; the G ponericins are like cecropins, W ponericins have similarities with gaegurins and melittin, and finally, L ponericins are similar to dermaseptins. All ponericins exhibit an α-helical structure in cell membranes [100].

The G family of ponericins share about 60% sequence similarity with cecropins. Cecropins exhibit broad spectrum antimicrobial activity against bacteria and fungi without affecting host cells [101-102]. The W family of ponericins have common properties due to their high sequence similarities. They are active against bacteria and yeast but also show hemolytic and insecticidal activities. Ponericins W have about 70% similarity in sequence to gaegurin 5 and melittin. Both the ponericin G and W families contain a Pro residue near the middle of the sequence in 11 of 13 sequences (the others G6 and G7 have the Pro residue near the C-terminus due to the shorter overall length). There have been studies performed on both G- and W-families of ponericins [103-108], along with novel peptides that show similarity to the G- and W-families [109-111].

The L-family ponericins, are the most poorly understood peptides and consist of ponericin L1 and L2. Both L1 and L2 share sequence similarities with dermaseptin 3 and 5 [112-114]. The only report of the activity and characteristics of these peptides are found in the original report by Orivel *et al.*, and even in this study, only ponericin L2 was examined. Ponericin L2 was shown to have broad-spectrum antibacterial activity with no hemolytic activity. The peptide adopted a random coil conformation in water (possibly polyproline-II helix). Ponericin L1 differs from L2 by only a single amino acid at position 9, with L1 containing a Met while L2 contains an Ile. There is

a general lack of understanding and investigation of the L-family of ponericins and their mechanism.

Role of cationic groups in AMPs. The cationic charge of an AMP is a key component in the initial binding between the peptide and the bacterial cell membrane [115]. However, many studies have shown that the position of cationic and hydrophobic residues can significantly impact the selectivity and antimicrobial activity of AMPs [116-120]. Therefore, the role of cationic residues in context of specific hydrophobic amino acids may also have an impact on activity. Cationic chain length tolerance may also be influenced by corresponding hydrophobic molecules' size and shape. This study focuses on the characteristics and behavior of ponericin L1 with extension to investigate the role of cationic residues and overall charge effects on activity.

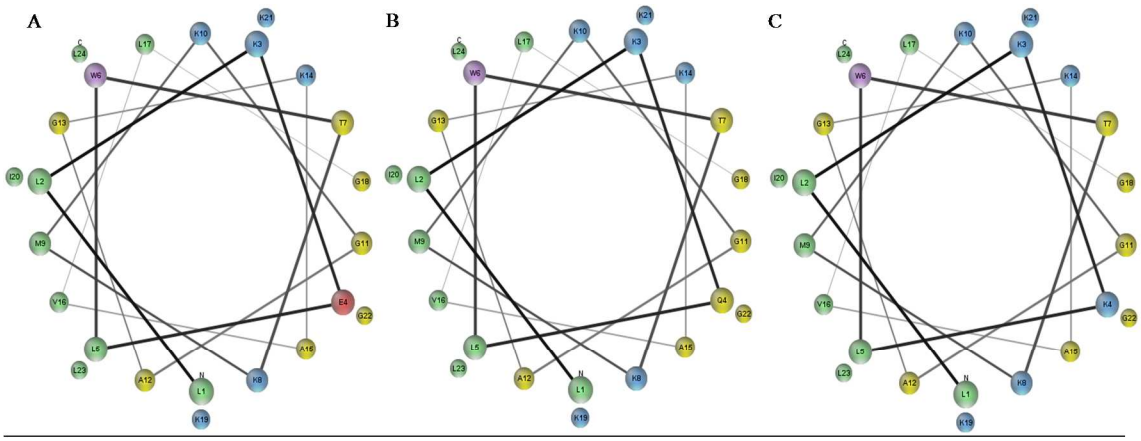

Peptide sequences, nomenclature, and properties

Name	Amino Acid Sequence	Net Charge	Molecular Weight (theoretical; Da)	Molecular Weight (found; Da)
L1	LLKELWTKMKGAGKAVLGKIKGLL	+5	2596	2594
L1-Q	LLKQLWTKMKGAGKAVLGKIKGLL	+6	2594	2594
L1-K	LLKKLWTKMKGAGKAVLGKIKGLL	+7	2595	2598
L1-R	LLRELWTRMRGAGRAVLGRIRGLL	+5	2763	2764
L1-O	LLOELWTOMOGAGOAVLGOIOGLL	+5	2512	2511
L1-X^D	LLXELWTXMXGAGXAVLGXIXGLL	+5	2344	2345

Figure 1. Peptide Sequences and Helical Wheel Diagrams. Helical wheel diagram of L1, A, L1-Q, B, and L1-K, C. Cationic residues are shown in blue, anionic in red, hydrophobic in green, polar uncharged in yellow, and aromatic are in purple. Peptides sequences and relevant properties are shown below the helical wheels. Helical wheel representations were made using MPEx [121]

Materials and Methods

Peptide preparation. Peptides L1-Q, L1-K, and L1-O (ornithine) were synthesized using standard FMOC-chemistry in-house. Peptide L1-R was purchased from Genscript (Piscataway, New Jersey). The peptide L1-X (L1 with lysine replaced with di-amino-propionic acid, Dap) presented significant synthetic challenges and was thus purchased from Synthetic Proteomics (Carlsbad, California) along with the L1 parent sequence. All peptides were subsequently purified via RP-HPLC using a Zorbax C3 column and eluted by a linear gradient of water to acetonitrile (both supplemented with 0.1% TFA). Peptide identity was confirmed using ESI-MS. HPLC fractions containing

peptide were pooled, lyophilized, and stored at −20°C. Prior to use, peptides were dissolved in 3:1 H2O:ethanol to create a stock solution of 150 to 200 μM and stored at 4°C.

Lipid preparation. Lipids 1,2-dioleoyl-sn-glycero-3-phosphocholine (DOPC; PC), 1,2-dioleoyl-sn-glycero-3-phospho-(10 -rac-glycerol) (DOPG; PG), and 1-palmitoyl-2-oleoyl-sn-glycero-3-phosphoethanolamine (POPE; PE) were purchased from Avanti Polar Lipids (Alabaster, Alabama), and stored as stocks in chloroform at −20°C. Lipids were prepared as 100% DOPC, 3:1 DOPC:DOPG (PC:PG), or 3:1 POPE:DOPG (PE:PG). Isopropyl β-D-1-thiogalactopyranoside (IPTG) (Chem-Impex Int'l INC.), ortho-nitrophenyl-β-galactoside (ONPG) (Research Products International Co.), nitrocefin (Biovision, Milpitas, California). All other chemicals and reagents were from Thermo Fisher Scientific (Waltham, Massachusetts), VWR (Radnor, Pennsylvania), or Sigma-Aldrich (St. Louis, Missouri). Small unilamellar vesicles (SUVs) were formed by sonication or by ethanol dilution methods. In all cases, appropriate volumes of lipids in chloroform were mixed in a glass test tube, dried under a gentle stream of N_2, and further dried under vacuum for at least 1 hour to create a lipid film in the tube. For the ethanol dilution vesicles, 10 μM of pure ethanol was added to the film, vortexed until the film was dissolved at which point the appropriate amount of PBS was added while vortexing. For sonicated vesicles, the PBS was added directly to the lipid film and vortexed to create multilamellar vesicles (MLVs). This MLV suspension was then subjected to sonication in a high-powered bath sonicator (Avanti Lipids) for 20 minutes to create SUVs.

Fluorescence spectroscopy. All fluorescence spectroscopy was performed on a JY-Horiba Fluoromax4 instrument with excitation and emission slit widths at 2.5 nm.

Measurements were taken in semi-micro quartz cuvettes. Spectral barycenters were calculated using the following formula: B = Pλ i Pi ð1Þ where B is the barycenter, λ is the wavelength, and i is the intensity at that wavelength. The summation is carried out over the entire emission spectrum collected, in this case 300 to 400 nm.

Binding experiments. Lipid binding assays were carried out as performed previously [122]. Briefly, the samples contained 2 μM peptide in PBS buffer (150 mM NaCl, 50 mM Na2HPO4; pH 7.0) and were titrated with a lipid vesicle stock (0.5 or 1.0 mM concentration). All binding assays used excitation at 280 nm and an emission range of 300 to 400 nm. The spectra were corrected from the background and the dilution after each addition.

Red-Edge Excitation Spectroscopy experiments. Red edge excitation shift (REES) experiments used excitation at 280, 290, 295, 300, 305, and 307 nm with an emission range of 310 to 410 nm. Again, samples contained 2 μM peptide in PBS buffer. The spectra were corrected from the background and the dilution after each addition.

TCE quenching. Trichloroethanol (TCE) quenching assays were performed by titrating 10 μL aliquots of 10 M TCE (Alfa Aesar, Haverhill, Massachusetts) into samples containing 2 μM peptide in PBS (150 mM NaCl, 50 mM Na2HPO4; pH 7.0). The Trp fluorescence emission was recorded after each addition with excitation at 280 nm and emission at 340 nm. Data were corrected from background and dilution. The Stern-Volmer quenching constant (Ksv) was determined from the slope of a linear best fit equation to the data.

Acrylamide quenching. Acrylamide quenching was performed by titrating 10 μL aliquots of 4 M acrylamide and measuring Trp emission after each addition. Samples contained 2 μM peptide and 250 μM total lipid in PBS. The Trp fluorescence emission was recorded after each addition with excitation at 295 nm and emission at 340 nm. Data were corrected for background, dilution, and inner filter effects in the excitation path as described previously [123]. The Ksv was calculated as above.

DQA experiments. Dual quencher analysis (DQA) experiments were performed as previously described [123]. Briefly, samples were prepared as above, with the exception that in one set of samples 10% of the lipid (molar basis) was replaced with the quencher 10-doxyl nonadecane (10-DN). Samples contained either no 10-DN (F0) or 20 μM 10-DN (Fdox). Similarly, peptide was added to a final concentration of 2 μM and allowed to equilibrate for 30 minutes. Fluorescence measurements were taken, and then 50 μL of acrylamide was added to each F0 sample, allowed to equilibrate, and remeasured. After inner filter correction (only for acrylamide containing samples) and background subtraction, the Q-ratio was calculated as previously described [123].

Circular dichroism spectroscopy. Circular dichroism (CD) spectra were collected using Jasco J-810 spectropolarimeter. Samples contained 5 μM peptide in 0.1X PBS buffer or 0.1X PBS buffer with 50% trifluoroethanol (Alfa Aesar). Lipid containing samples consisted of 200 μM lipid vesicles with 3 μM peptide in 0.1X PBS buffer. Each sample had 64 scans performed with correction from background without peptide.

Bacterial culturing. Bacteria were streaked on LB-Miller agar plates from a frozen glycerol stock made from the original samples shipped from CGSC (Coli Genetic

Stock Center, Yale University) or ATCC (American Type Culture Collection) (Escherichia coli D31 CGSC 5165 [124], Staphylococcus aureus ATCC 35556, Pseudomonas aeruginosa PA-01 ATCC 47085 [125], Acinetobacter baumannii ATCC 19606). An overnight was prepared using a single colony of each bacterial strain into fresh LB broth and placed into a shaking incubator 37 C at 225 rpm for ~18 hours. After incubating overnight, a fresh 1:200 dilution was made in LB broth and used for the experiment.

Minimal Inhibitory Concentration (MIC)/Minimal Bactericidal Concentration (MBC). Minimum inhibitory concentration (MIC) was performed using mid-log phase bacteria diluted to 5 × 105 CFU/mL. Then, 90 μL of the diluted culture was added to the wells of a sterile 96-well plate containing serially diluted aliquots of each peptide for a total volume of 100 μL. The plate was incubated at 37 C for 18 hours. After incubation, bacterial growth was determined by measuring OD600 using a Spectramax M5 multimode plate reader. Minimum bactericidal concentration (MBC) was performed by removing 1 μL of culture from each well of the MIC plate and plating on a fresh LB agar plate which was subsequently incubated overnight at 37 C. MBC was determined by the growth or absence of growth from each well on the agar plate.

Lipid vesicle leakage. Lipid films were prepared as described above. A 75 mM stock of calcein was prepared in HEPES buffer, pH 7. The lipid film was resuspended in 700 μL of calcein solution for a final lipid concentration of 20 mM. The resuspended lipid vesicle sample was subjected to seven freeze-thaw cycles by alternating between a liquid N_2 bath and a 42 C water bath, culminating with a final thaw of the sample. The vesicles were then sonicated using a VCX 130 Probe sonicator (Sonics & Materials, Inc.)

for 1 minute, using 1 second pulses at 45% intensity. Vesicles were separated from unincorporated calcein by size exclusion chromatography using G25 Sephadex. The column was equilibrated in HBS (50 mM HEPES, 150 mM NaCl, pH 7) under gravity flow for approximately 1 hour before the vesicle solution was loaded onto the column. Upon loading, ~40 1 mL Fractions were then collected from the column. Fractions containing vesicles with entrapped calcein exhibited a cloudy, orange color and were separated from the unincorporated calcein, which has a clear yellow color. Vesicles were used on the same day as prepared. Vesicle concentrations/dilution factor were determined using a ratiometric assay with vesicles containing a known concentration of fluorescent lipid [126]. The two most concentrated fractions were diluted 1:1 with HBS buffer. Solutions were dispensed into a 96 well plate in the subsequent order: 10 μL of peptide with serial dilutions starting at a final concentration from 15 μM (excluding the last row which had 10 μL of 0.01% Acetic Acid as a negative control), 20 μL of the diluted vesicle fractions, and 70 μL of PBS buffer (50 mM sodium phosphate, 150 mM sodium chloride pH 7) for a final lipid concentration of ~200 μM. The samples were excited at 495 nm and fluorescence emission was measured at 520 nm using a 510 nm cutoff filter in a Spectramax M5 (Molecular Devices) multimode plate reader. Following the initial reading, 20 μL of Triton X-100 was added the last row as a positive control. The plate was placed on a plate shaker for 1 hour at 400 rpm, shielded from light. Calcein fluorescence emission was then remeasured and used as the 100% leakage normalization value. Data reported are the average of three replicates.

Bacterial inner membrane permeabilization assay. An overnight culture of E. coli D31 was prepared by inoculating a single colony into fresh LB broth and placed in a

37 C shaking incubator (225 rpm) for ~18 hours. Following the overnight incubation, a 1:250 dilution of the culture to fresh LB broth was made. This was supplemented with 100 μL of 100 mM IPTG to induce the expression of β-galactosidase. The dilution was incubated with shaking until an OD600 of 0.2 to 0.4 was reached. Solutions were dispensed into a 96 well plate in the subsequent order: 10 μL of peptide with serial dilutions starting a final concentration from 15 μM (excluding the last row which had 10 μL of 0.01% acetic acid as a negative control), 56 μL Z-buffer (60 mM Na2HPO4, 40 mM NaH2PO4, 10 mM KCl, 1 mM MgSO4, 50 mM β-mercaptoethanol, pH 7), 19 μL of E. coli culture, and 15 μL of 4 mg/mL ONPG dissolved in Z-buffer. Immediately following the addition of ONPG, absorbance was recorded at 420 nm every 5 minutes for 90 minutes. The detergent cetyltrimethylammonium bromide was added in place of the peptide as a positive control. Data reported are the average of three replicates.

Bacterial outer membrane permeabilization assay. An overnight culture of E. coli D31 was prepared by inoculation a single colony into fresh LB broth with 100 μg/mL ampicillin (LB-Amp) and placed in a 37 C shaking incubator (225 rpm) for ~18 hours. Following the overnight incubation, a 1:250 dilution of the culture to fresh LB-Amp was made. The dilution was incubated with shaking until an OD600 of 0.2 to 0.4 was reached. The bacterial culture was then centrifuged at 2500 rpm for 15 minutes in a tabletop clinical centrifuge. The supernatant was discarded and the pellet was resuspended in an equal amount of PBS (100 mm NaH2PO4, 200 mM NaCl, pH 7). The experimental samples were prepared in a 96 well plate in the subsequent order: 10 μL of peptide with serial dilutions starting at a final concentration from 15 μM (excluding the last row which had 10 μL of 0.01% acetic acid as a negative control), 80 μL of the

resuspended E. coli culture, and 10 μL of 50 μg/mL Nitrocefin in PBS. Immediately following the addition of nitrocefin, absorbance was recorded at 486 nm every 5 minutes for 90 minutes. The antimicrobial polymyxin B was used as a positive control. Data reported are the average of three replicates.

Hemolysis assay. Hemolysis of human red blood cells (RBCs) was used to quantify membrane destabilization by leakage of hemoglobin. Blood was collected in vacutainer tubes (10 mL) with EDTA coating as an anticoagulant (provided by the Rowan Department of Health and Exercise Science from a fresh draw ~1 hour prior to use, IBC protocol 2019-11). A 7 mL aliquot of whole human blood was mixed with 7 mL of sterile PBS. The solution was then sedimented via centrifugation for 7 minutes at 2500 rpm. The supernatant was removed and the pellet containing RBCs was resuspended to the original volume of 14 mL with PBS. This process was repeated three times. The final cell pellet was resuspended to a final volume of 14 mL and 90 μL of this cell suspension was added to all wells of a conical-bottom 96-well plate. Prior to addition of RBCs, 10 μL of serially diluted peptide or the detergent Triton-X 100 (as a positive control) were added to the wells. The covered plate was placed into a shaking incubator for 60 minutes at 37 C while shaking (150 rpm). The conical plate was centrifuged for 10 minutes at 200 rpm and 4 C. Subsequently, 6 μL of the supernatant was added to 94 μL of fresh PBS in wells of a flat-bottom plate. Analysis of hemolysis was performed by measuring absorbance at 415 nm using a Molecular Devices Spectramax M5 plate reader. Percent hemolysis was calculated based on the absorbance of each well compared to those wells with no additive and those with Triton-X 100. All data reported are the average of three replicates.

Results

Peptides. The original L1 sequence and all of the variants tested are listed with net charge, and molecular mass in Figure 1. Standard amino acid abbreviations are used except in the case of L1-O and L1-X, which represent the cationic substitutions of lysine with ornithine or di-amino-propionic acid, respectively. Solid-phase FMOC chemistry methods were used to synthesize all peptides. Peptides were purified using HPLC. The helical wheel diagrams depict the orientation of amino acids along the helical axis, also shown in Figure 1. In general, the original L1 sequence does not adopt a canonical amphiphilic helix with a hydrophobic face and a cationic face. Instead the L1 peptide in helical conformation exhibits a hydrophilic face, but the cationics are flank that face with a number of polar, uncharged, and the lone anionic group interspaced on this face. Like L1, numerous venom peptides do not have a strictly cationic face, but instead a polar face with cationic and polar uncharged residues [127-129].

Antimicrobial activity. Antimicrobial activity of L1 and variants were tested using a broth microdilution assay to determine the MIC (Table 1). All peptides exhibited similar (fourfold range) of activity against *E. coli*, and all but L1-X showed similar activity against *A. baumannii*. In contrast, the parent L1 sequence showed weak activity against *S. aureus* and *P. aeruginosa*, while L1-R, L1-Q, and L1-K were more effective against *S. aureus*, while L1-K and L1-Q were also very active against *P. aeruginosa*. The concentration required to kill the bacteria in solution, or MBC, was also measured by a plating assay after the MIC assay. The MBC values for each peptide was equal to or about 2x greater than the MIC. These results indicate that the L1 peptides are likely acting in a bactericidal mechanism, instead of a bacteriostatic mechanism. A bactericidal

mechanism is assumed because the bacteria is not growing when removed from the antimicrobial peptide solution and placed on a fresh LB-agar plate.

Table 1

MIC and MBC (μM)

	E.coli		***S. aureus***		***P. aeruginosa***		***A. baumannii***	
	MIC	**MBC**	**MIC**	**MBC**	**MIC**	**MBC**	**MIC**	**MBC**
L1	0.94	0.94	15.00	15.00	15.00	15.00	1.88	1.88
L1-Q	0.94	0.94	1.88	1.88	7.50	7.50	0.94	1.88
L1-K	1.88	1.88	3.75	3.75	3.75	3.75	0.94	0.94
L1-R	0.94	0.94	1.88	1.88	15.00	15.00	0.94	1.88
L1-O	1.88	1.88	>15	>15	15.00	15.00	1.88	1.88
L1-X	3.75	7.50	>15	>15	15.00	>15	>15	>15

Note: Abbreviations: MIC, minimal inhibitory concentration; MBC, minimal bactericidal concentration.

Solution behavior. The antimicrobial activity of most AMPs begin with the peptide in solution before interacting with the bacterial membrane, including the L1 peptide. Behavior of the peptide in solution and how sequence variation can affect these properties play a role in the equilibrium between the free and bound states of the peptide. Red-Edge Excitation Spectra (REES) can be used to indicate the mobility of the Trp fluorophore, and yield insights into relative changes in the peptide aggregation and/or oligomerization [130-131]. REES results are shown in Figure 2A. All peptides displayed some extent of increase in the spectral barycenter as a function of excitation wavelength.

This indicates some level of restricted motion around the Trp fluorophore. The L1, L1-K, L1-R, and L1-X sequences showed significant shifts in the emission, between 7 and 11 nm at the highest excitation wavelength (307 nm), shown in the inset of Figure 2A. The red edge effects at this magnitude are strongly indicative of restricted motion around the Trp, likely caused from peptide aggregation or oligomerization.

Quenching of Trp fluorescence by TCE was also performed to investigate the aggregation of L1 and variants. TCE has been shown to partition the interior of protein aggregates and quench Trp more efficiently at the interior of these aggregates. The Stern-Volmer quenching constant, otherwise referred to as Ksv, is calculated from the slope of a linear fit to the quenching data, and was used to analyze the quenching. A higher Ksv value indicates increased Trp quenching. TCE quenching pattern determined by Ksv is shown in Figure 2B (as well as Table 2). Comparing results of TCE to REES there is some difference. L1-X and L1-K, which showed significant REES were also strongly quenched by TCE. On the other hand, L1 and L1-R, which also showed significant REES, were only minimally quenched by TCE. These results indicate potential differences in the packing or organization of the L1 solution aggregation state as a function of the sequence.

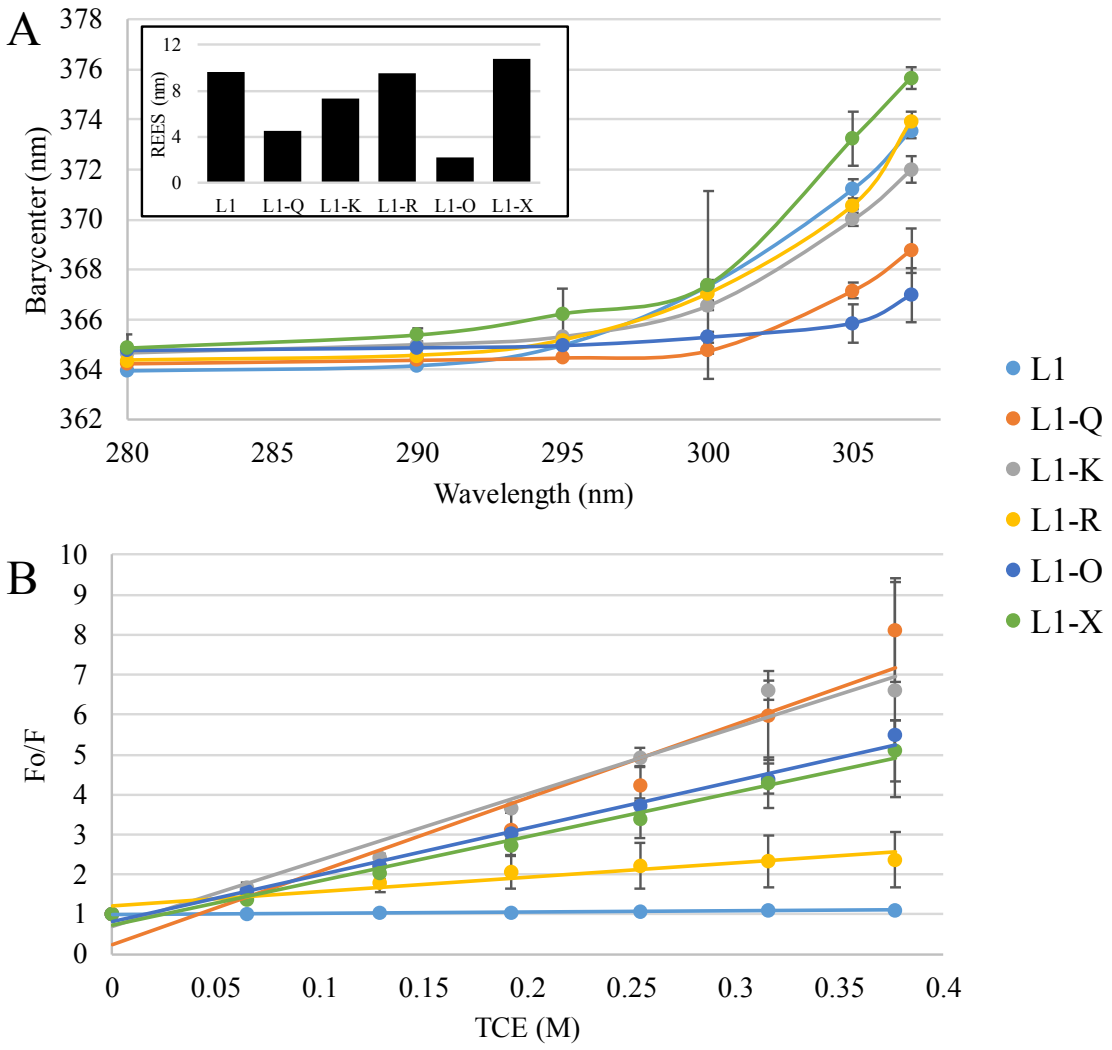

Figure 2. Peptide Solution Assays. Red-edge excitation shift (REES), A, and trichloroethanol (TCE) quenching, B. The inset in panel A depicts the total shift for each peptide. In both panels, L1 is shown in light blue, L1-Q in orange, L1-K in gray, L1-R in yellow, L1-O in dark blue, and L1-X in green. All data are averages of three samples with correction from the background and error bars represent the SD.

Table 2

TCE Quenching

Sequence	Ksv (M^{-1})		
L1	0.30	±	0.04
L1-Q	15.35	±	3.75
L1-K	17.63	±	1.21
L1-R	4.23	±	2.78
L1-O	10.97	±	1.25
L1-X	10.50	±	2.53

Interactions with lipid bilayers. A critical early step in the widely accepted membrane-permeabilization mechanism for AMPs is the peptide interaction with lipid bilayers. The affinity and orientation of membrane interacting peptides has been shown to be impacted by bilayer thickness, headgroup composition, pH, and other factors. As compared to a traditional host defense peptide, L1 is a venom-derived peptide and despite its net positive charge there is no inherent evolutionary need for it to preferentially interact with anionic bilayers.

Affinity for lipid bilayers was investigated using the environmental sensitivity of the naturally occurring Trp residue in the L1 sequence. When the local environment around the Trp shifts from more polar (aqueous solution) to less polar (surface of the bilayer or imbedded in bilayer core), the Trp fluorescence emission spectrum exhibits a shift from “red” to “blue”. The shift of the spectrum is determined by the shift in the spectral barycenter, or center of mass, as a function of titrated lipid vesicles [115]. The spectral barycenter was calculated using the intensity-weighted average over the range

wavelengths collected [132]. The data from these binding experiments are shown in Figure 3, with representative spectra of the free and bound peptides shown in Figure 4. All variants exhibited binding to all lipid compositions tested (100% PC; 3:1 PC:PG; 3:1 PE:PG; and 7:3 PC:Cholesterol). Higher binding affinity was shown to bilayers containing anionic lipids (note the difference in X-axis scaling in Panels A and C vs B and D in Figure 3). The peptide L1-X, containing the shortest side chain, exhibited a lower total shift in barycenter when completely bound in all lipids, indicating this substitution affects the depth of insertion into the bilayer. Although there was a lower total shift, it did not seem to have an effect on the general affinity for vesicles with anionic lipids.

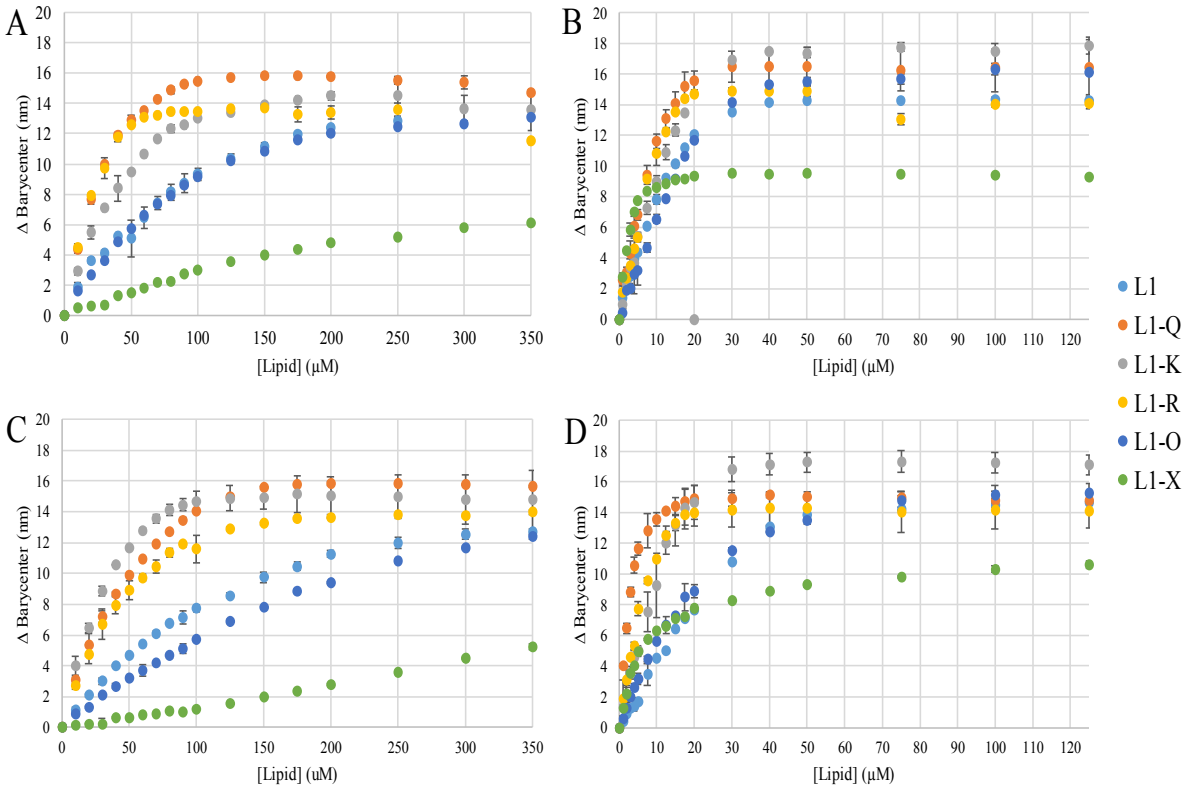

Figure 3. Binding to Lipid Vesicles. Peptide binding was assayed using Trp fluorescence emission by titrating SUVs into a sample containing 2 μM peptide. The spectral barycenter was calculated after each addition of lipid vesicle and the Δbarycenter is the difference between the initial barycenter and that after each addition. Binding was assayed with, A, PC, B, 3:1 PC:PG, C, 3:1 PC:Cholesterol, and, D, 3:1 PE:PG. In all panels, L1 is shown in light blue, L1-Q in orange, L1-K in gray, L1-R in yellow, L1-O in dark blue, and L1-X in green. Note the difference in X-axis scaling for panels A and C vs B and D. All data are averages of three replicates and the error bars represent the SD.

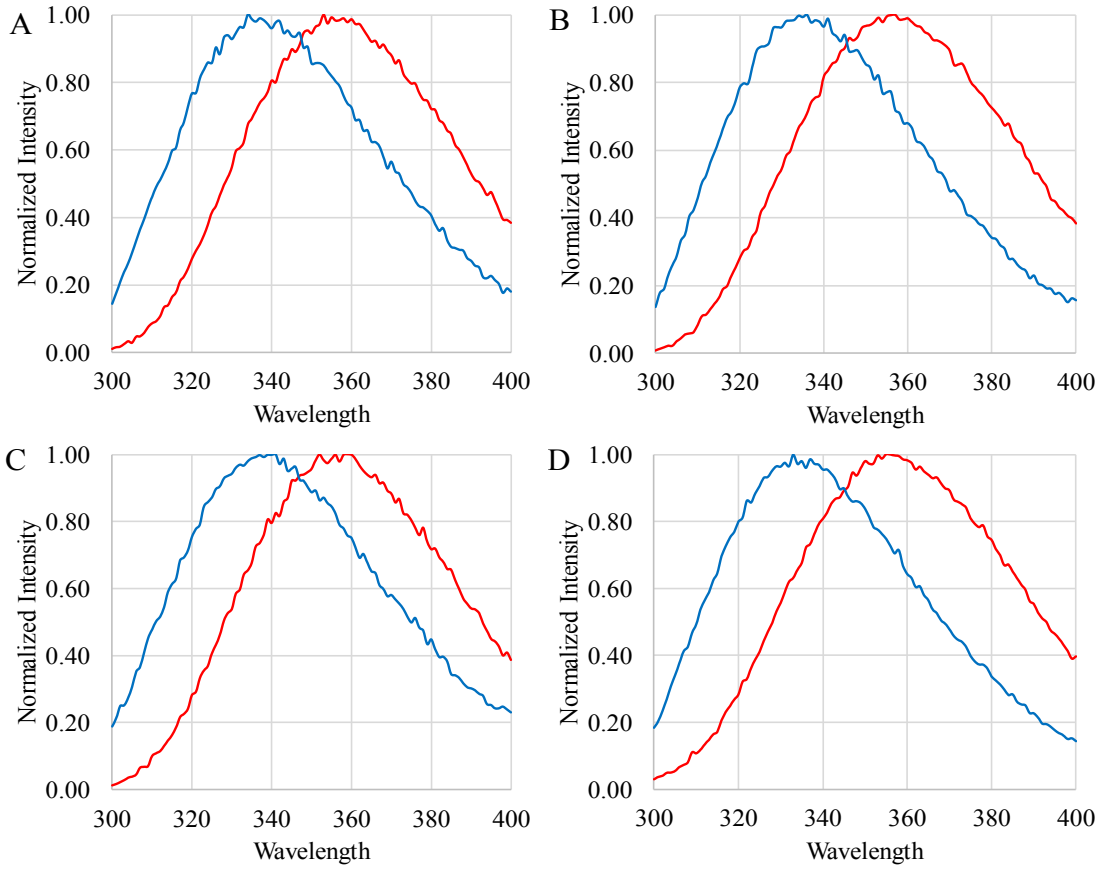

Figure 4. Normalized Trp Emission Spectra. L1 peptide data shows before (red) and after (blue) interacting with lipid vesicles. Data are representative spectra after subtraction of a background spectrum. All samples contained 2 μM peptide and 300 μM lipid □ (A) PC, (B) PC:PG, (C) PC:Chol, (D) PE:PG.

A series of fluorescence quenching experiments were performed to further investigate how the peptides interact with bilayers. Acrylamide quenching was performed on the peptides in solution and when bound to bilayers with various composition. Trp residues that are exposed to the aqueous environment are quenched efficiently by acrylamide. Acrylamide will not quench Trp buried in the nonpolar core of the bilayer. Thus, the quenchability of the Trp is directly related to its exposure to the aqueous environment. The Stern-Volmer, or K*sv*, quenching constants for the L1 peptides

quenched by acrylamide under different conditions are shown in Table 3, with full quenching profiles shown in Figure 5. To calculate the K*sv*, the equation used is: $\frac{F^0}{F} = 1 + K_{sv}[Q]$, where F^0 is the fluorescence intensity in the absence of the quencher Q, and F is the fluorescence intensity in the presence of different concentration of Q. The constant *Ksv* is the product of the true quenching constant k_q, and the fluorescence lifetime in the absence of the added quencher, τ_0 [133]. In all conditions, the peptides show a decrease in the K*sv* between aqueous and any bilayer-interacting condition, supporting the binding results showing the peptides interact with all bilayers.

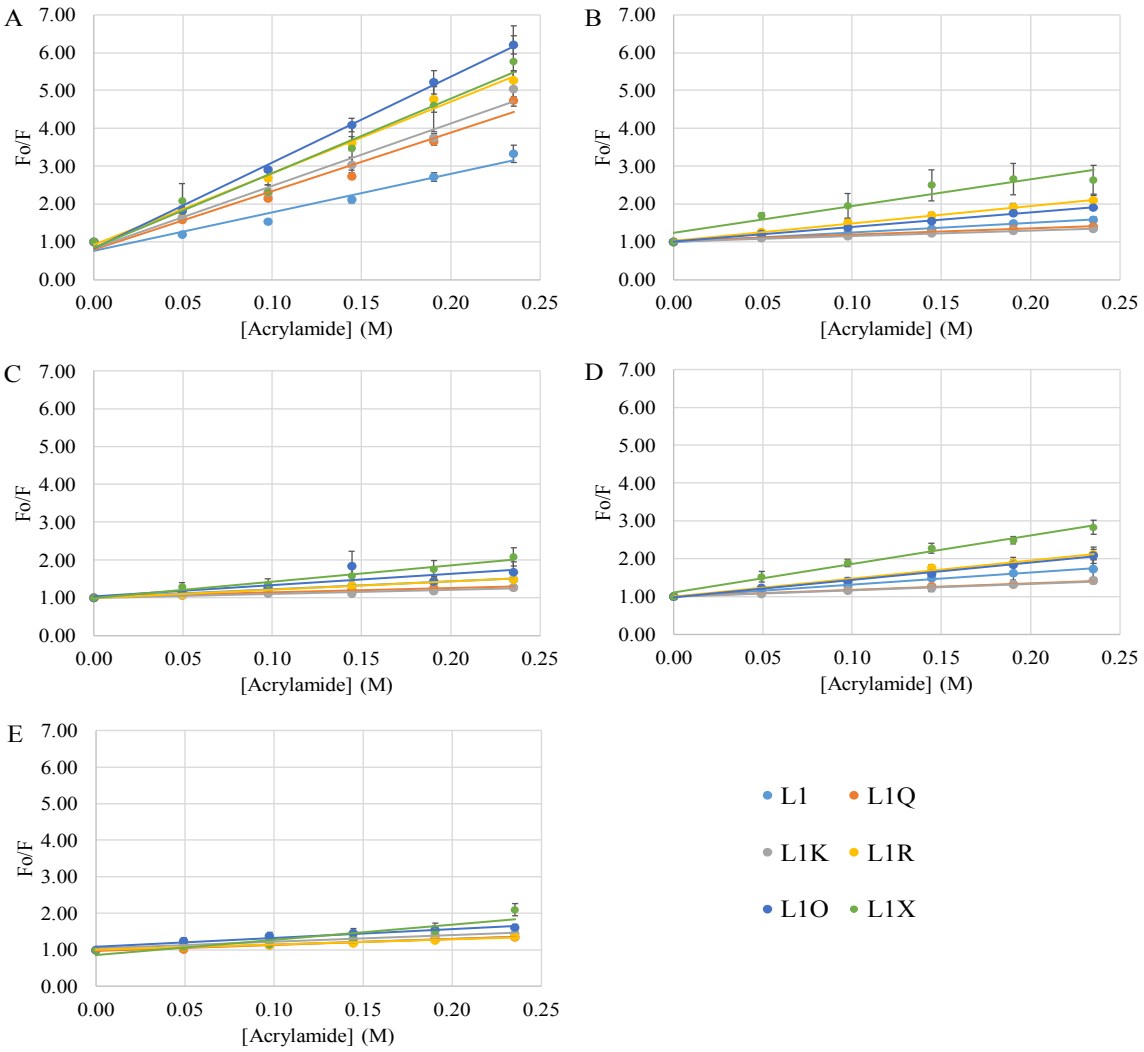

Figure 5. Acrylamide Quenching of L1 Peptides. Data shows L1 peptides in (A) PBS buffer, (B) PC vesicles, (C) PC:PG vesicles, (D) PC:Chol vesicles or (E) PE:PG vesicles. All samples contained 2 μM peptide and 250 μM lipid (for those with vesicles). Data are corrected for inner filter effects and are background subtracted. Data represent the average and SD of 3□6 samples.

Table 3

Fluorescence Quenching

	Acrylamide Quenching (Ksv (M^{-1}))						Q-Ratio		
	PBS	*DOPC*	*PC/PG*	*PC/PG/PE*	*PC/Chol*	*PE/PG*	*DOPC*	*PC:PG*	*PE:PG*
L1	10.14 ± 1.15	2.49 ± 0.32	2.08 ± 0.27	1.89 ± 0.28	3.18 ± 1.27	1.51 ± 0.08	3.46	1.29	0.15
L1-Q	15.43 ± 0.17	1.67 ± 0.19	1.23 ± 0.01	1.52 ± 0.25	1.72 ± 0.16	1.63 ± 0.08	1.68	2.12	0.80
L1-K	16.48 ± 1.97	1.44 ± 0.13	1.07 ± 0.07	1.13 ± 0.63	1.77 ± 0.37	1.86 ± 0.01	4.09	2.51	1.78
L1-R	18.90 ± 1.49	4.64 ± 0.65	2.20 ± 0.21	0.60 ± 0.27	4.82 ± 0.81	1.46 ± 0.23	3.13	0.13	1.00
L1-O	22.68 ± 0.84	3.86 ± 0.09	2.96 ± 1.40	0.46 ± 0.63	4.54 ± 1.14	2.47 ± 0.39	4.01	1.86	1.41
L1-X	19.69 ± 4.29	7.09 ± 2.38	4.28 ± 1.17	4.72 ± 0.33	7.56 ± 0.20	4.17 ± 0.72	4.08	1.86	7.16

Note: Abbreviations: DOPC, 1,2-dioleoyl-sn-glycero-3-phosphocholine; DOPG, 1,2-dioleoyl-sn-glycero-3-phospho-(10 -rac-glycerol). Data are averages of three to six replicates with SD.

An extension of the acrylamide quenching assay is the DQA assay, which utilizes acrylamide and a second, membrane-imbedded quencher, 10-DN. Although, acrylamide is a widely used quencher of Trp, it is unable to efficiently quench the fluorescence of Trp residues that are deeply submerged in the core of a bilayer [134-135]. This is why the novel Trp quencher, 10-DN is used alongside acrylamide. 10-DN is a highly hydrophobic molecule that contains a nitroxide-bearing doxyl group, which helps it strongly quench Trp fluorescence [136-137]. The ratio of quenching between each quencher is directly dependent on the Trp depth in the bilayer, which can help determine the orientation in the bilayer. This can qualitatively identify orientation differences between different bilayer compositions [123]. In the DQA assay, the more exposed the Trp residue is to the

aqueous environment, the higher the Q-ratio. All Q-ratios for the L1 variants are shown in Table 3, with visuals in Figure 6. The Q-ratio for all peptides in DOPC were similar, regardless of sequence or affinity, but lower values were shown for peptides in bilayers with anionic lipids, except L1-X in PE:PG bilayers.

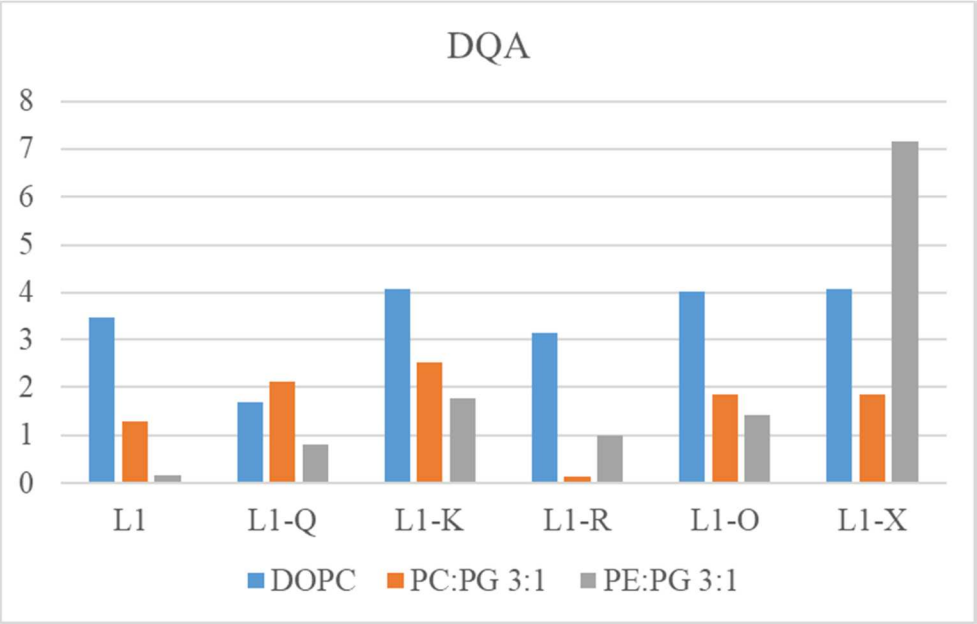

Figure 6. Dual Quencher Analysis of L1 Peptides. Q-ratios were calculated for peptides bound to lipid vesicles containing DOPC (blue), 3:1 DOPC:DOPG (orange), or 3:1 POPE:DOPG (grey) bilayers. The Q-ratio is calculated from the ratio of F_0/F values for quenching by 10-doxyl nonadecane and acrylamide at fixed concentrations. F_0/F values are averages of three to five samples.

A fluorescent dye-release assay was used to investigate the ability of each peptide to permeabilize model lipid vesicles. The fluorophore calcein undergoes self-quenching when entrapped in the lumen of the vesicle, which exhibits low fluorescence emission

increasing dramatically upon bilayer permeabilization and release of the fluorophore into the aqueous surrounding. Peptides were exposed to lipid vesicles composed of PC, PG:PG, or PE:PG lipid mixtures. The percent leakage was calculated based off a subsequent treated of the vesicles with the bilayer disrupting detergent, Triton X-100. Leakage data is shown in Figure 7. The L1 peptides, in all lipid compositions, did not induce leakage to a large extent, however at the highest concentration tested, L1, L1-R, and L1-Q induced up to ~ 15% leakage in vesicle that contained PC. Interestingly, none of the peptides induced any discernable leakage in vesicles composed of PE:PG lipids which are commonly found in bacterial membranes.

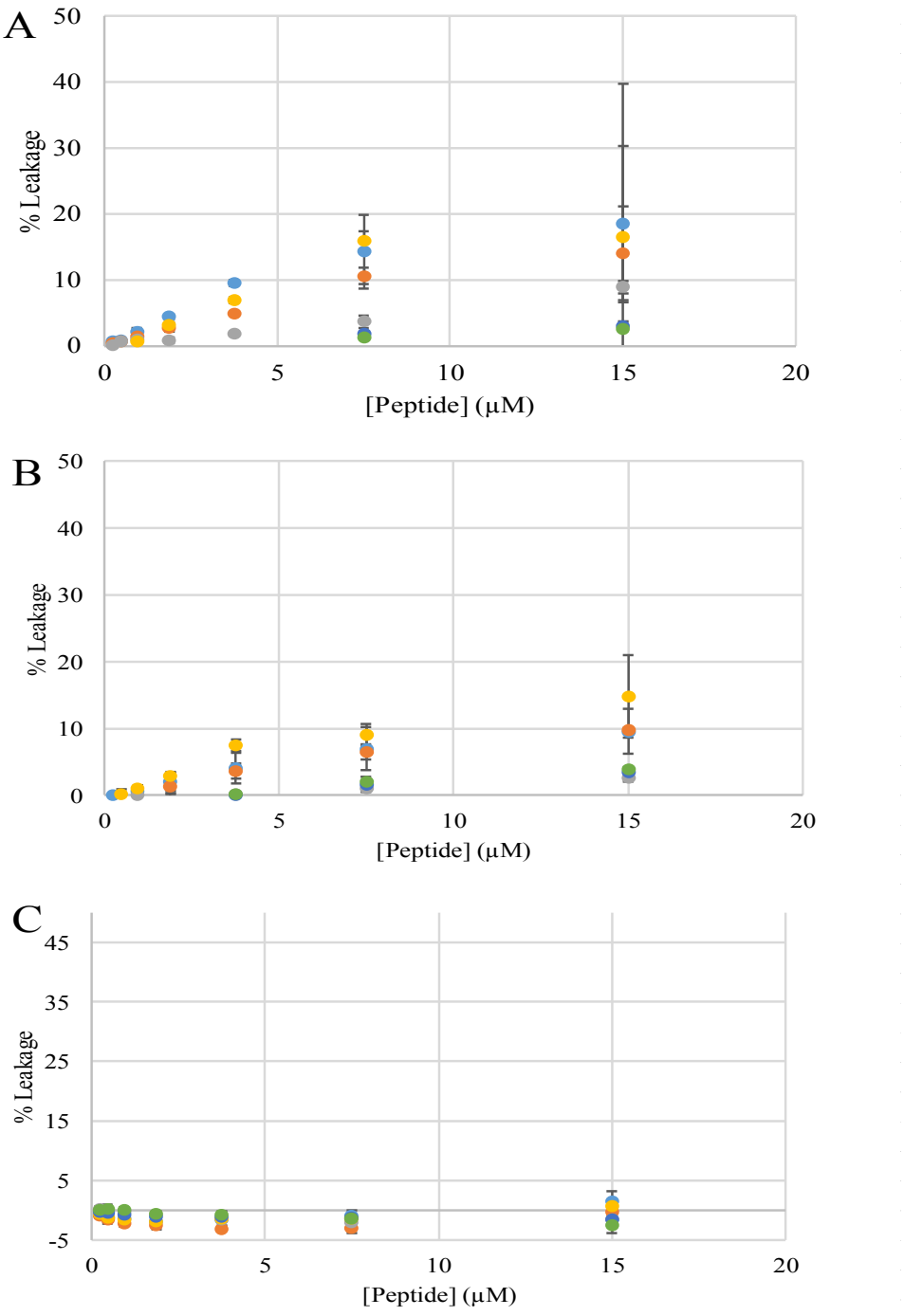

Figure 7. Vesicle Permeabilization Assays. Peptide permeabilization of model lipid vesicles determined by dye leakage assays using calcein. Vesicles were composed of, A, PC, B, 3:1 PC: PG, C, 3:1 PE:PG. In all panels, data were normalized based on untreated vesicles (0% leakage) and vesicles treated with the detergent Triton X-100 (100% leakage). L1 is shown in light blue, L1-Q in orange, L1-K in gray, L1-R in yellow, L1-O in dark blue, and L1-X in green. All data are averages of at least three replicates and the error bars represent the SD.

Interactions with cellular membranes. L1 peptides were investigated for the ability to permeabilize natural bacterial and mammalian membranes. Peptide interactions with model lipid vesicles is informative; however, model vesicles only replicate a small fraction of the complexity of natural lipid membranes which inherently contain greater lipid diversity, lipid asymmetry, and integral membrane proteins. Using chromogenic substrates of enzymes localized in the *E. coli* periplasmic space (nitrocefin and β-lactamase) or cytoplasm (ONPG and β-galactosidase), the peptide effects on the permeability of the bacterial outer or inner membrane can be investigated. Outer membrane permeability is shown in Figure 8A while inner membrane permeability is shown in Figure 8B. Notably, these data represent snapshots of leakage after 30 minutes of exposure to the peptides, but full 90-minute time course data is shown in Figure 9 (Outer membrane) and Figure 10 (Inner Membrane). All peptides exhibited the ability to disrupt the outer membrane in a concentration dependent manner, although L1-X only did so at the highest concentration tested (Figure 8A). None of the peptides induced any significant permeabilization of the E. coli inner membrane other than L1-R at the highest concentrations tested (Figure 8B).

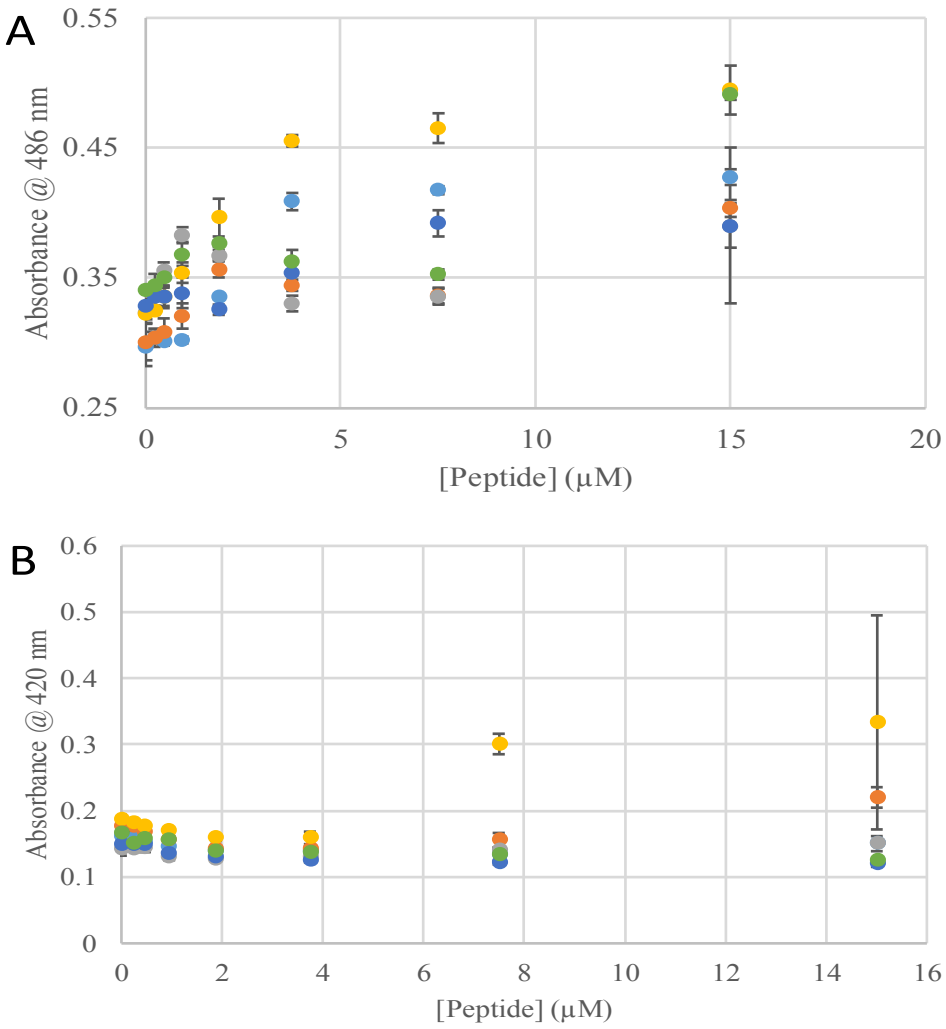

Figure 8. Membrane Permeabilization of *E. coli*. *E. coli*, A, outer membrane and, B, inner membrane permeabilization. L1 is shown in light blue, L1-Q in orange, L1-K in gray, L1-R in yellow, L1-O in dark blue, and L1-X in green. All data are averages of at least three replicates and error bars represent the SD. In some cases, error bars are smaller than the size of the symbols.

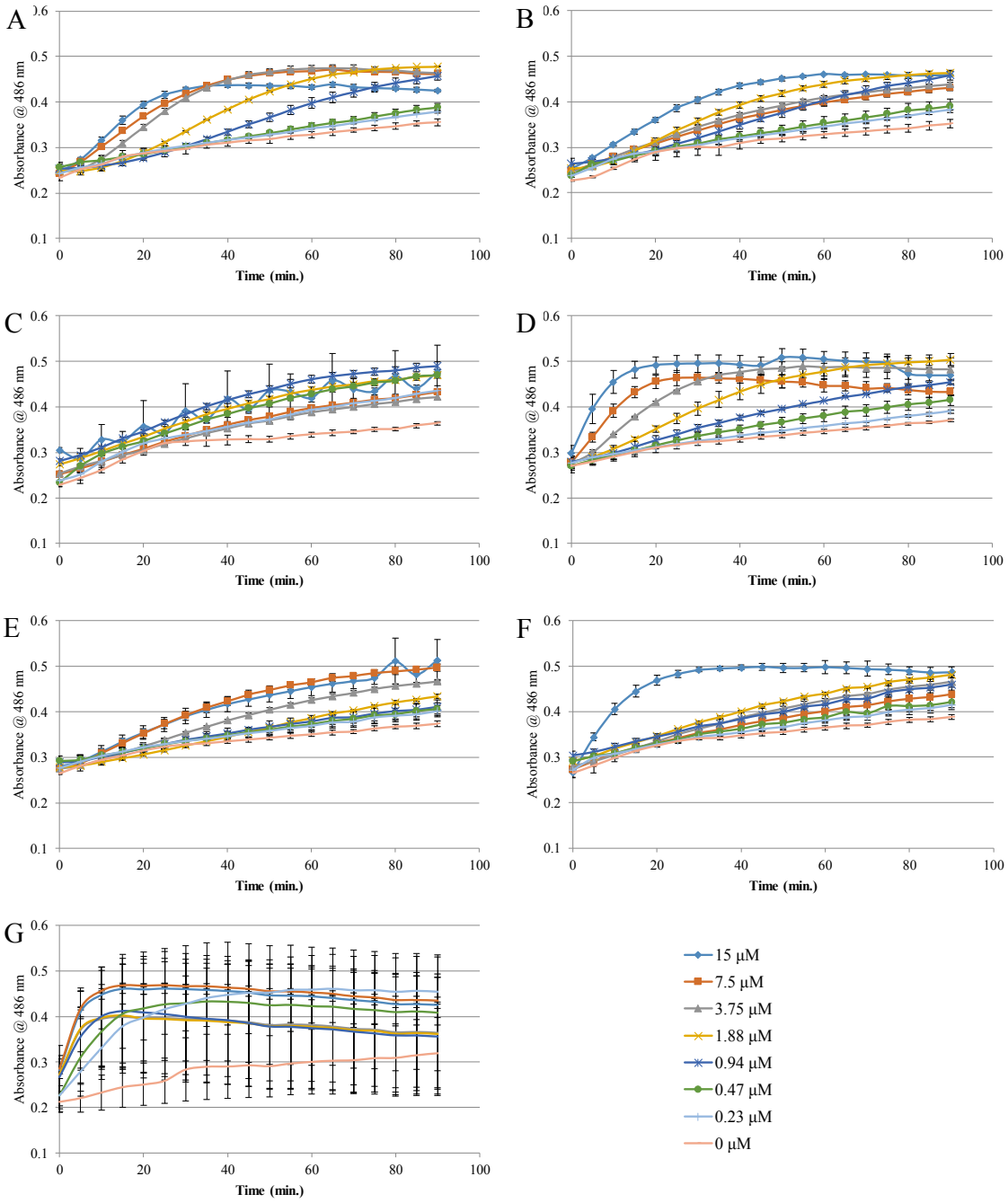

Figure 9. *E. coli* Outer Membrane Permeabilization Assay. Absorbance at 486 nm represents the breakdown of the nitrocefin substrate by the periplasmic enzyme β□ lactamase. Bacteria were exposed to varying concentrations of peptide and the corresponding colors for each panel are shown in the legend. (A) L1, (B) L1□Q, (C) L1□K, (D) L1□R, (E) L1□O, (F) L1□X, (G) Polymyxin B. Data represent the average and SD of 3□6 samples.

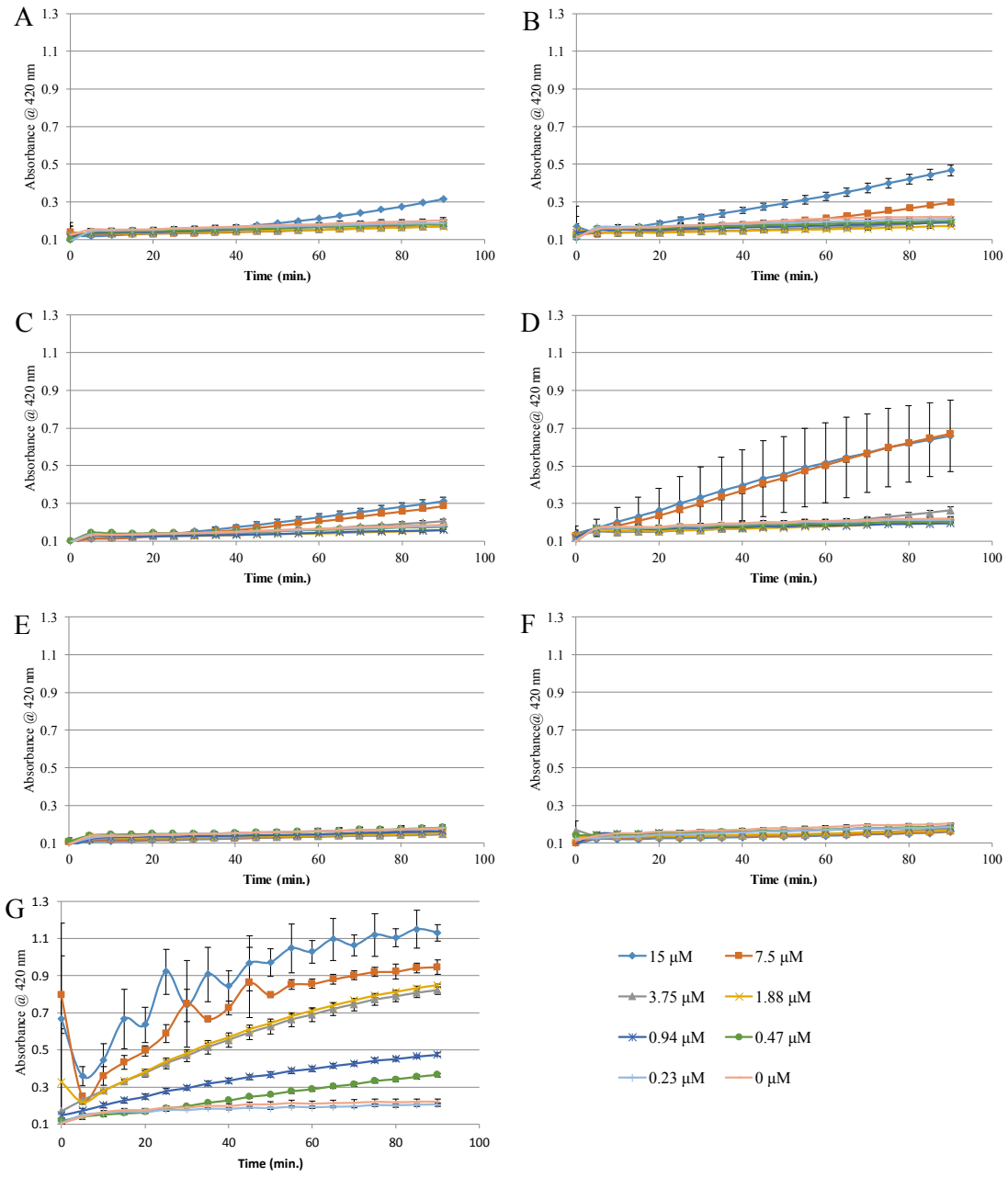

Figure 10. E. coli Inner Membrane Permeabilization Assay. Absorbance at 420 nm represents the breakdown of the ONPG substrate by the periplasmic enzyme β□ galactosidase. Bacteria were exposed to varying concentrations of peptide and the corresponding colors for each panel are shown in the legend. (A) L1, (B) L1□Q, (C) L1□ K, (D) L1□R, (E) L1□O, (F) L1□X, (G) cetyltrimethylammonium bromide (CTAB). Data represent the average and SD of 3□6 samples.

Although bacterial membrane permeabilization may be linked to antimicrobial activity; the L1 peptides have been shown to also permeabilize mammalian membranes. It is critical to understand if L1 peptides can kill host cells, which is why a hemolysis assay was performed. The ability to disrupt human RBC membranes was investigated using a hemolysis assay monitoring the release of hemoglobin after exposure to the peptides for 1 hour. Percent leakage was calculated based on a subsequent treatment of the RBCs with the bilayer disrupting detergent Triton X-100. The results are shown in Figure 11, with none of the L1 peptides inducing any significant disruption of RBCs, consistent with the previously published results on the related L2 peptide [99].

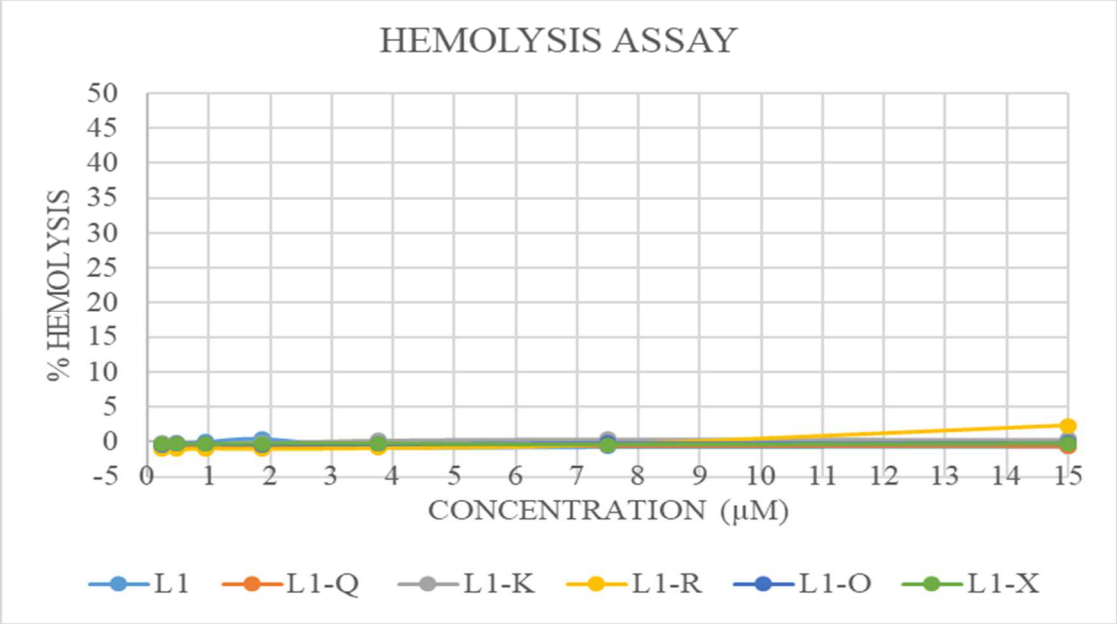

Figure 11. Hemolysis of Human Red Blood Cells (RBCs). Hemolysis of RBCs. Data were normalized based on untreated RBCs (0% hemolysis) and RBCs treated with the detergent Triton X-100 (100% hemolysis). L1 is shown in light blue, L1-Q in orange, L1-K in gray, L1-R in yellow, L1-O in dark blue, and L1-X in green. All data are averages of at least three replicates and error bars represent the SD. In some cases, error bars are smaller than the size of the symbols.

Peptide secondary structure. The changes in amino acid sequence can inherently impact the structure that the peptides adopt in solution or when bound to membranes. Due to their small size, the L1 peptides are unlikely to adopt any tertiary structures, so secondary structure analysis by CD spectroscopy provides a good picture of the overall peptide structure. CD spectra of the L1 peptides in phosphate buffer alone or in buffer with 3:1 PC:PG vesicles are shown in Figure 12. In aqueous solution, all peptides exhibit CD spectra consistent with random / disordered structures except L1-O which exhibits a helical signature. When bound to lipid vesicles, all variants exhibited spectra indicative of α-helix formation.

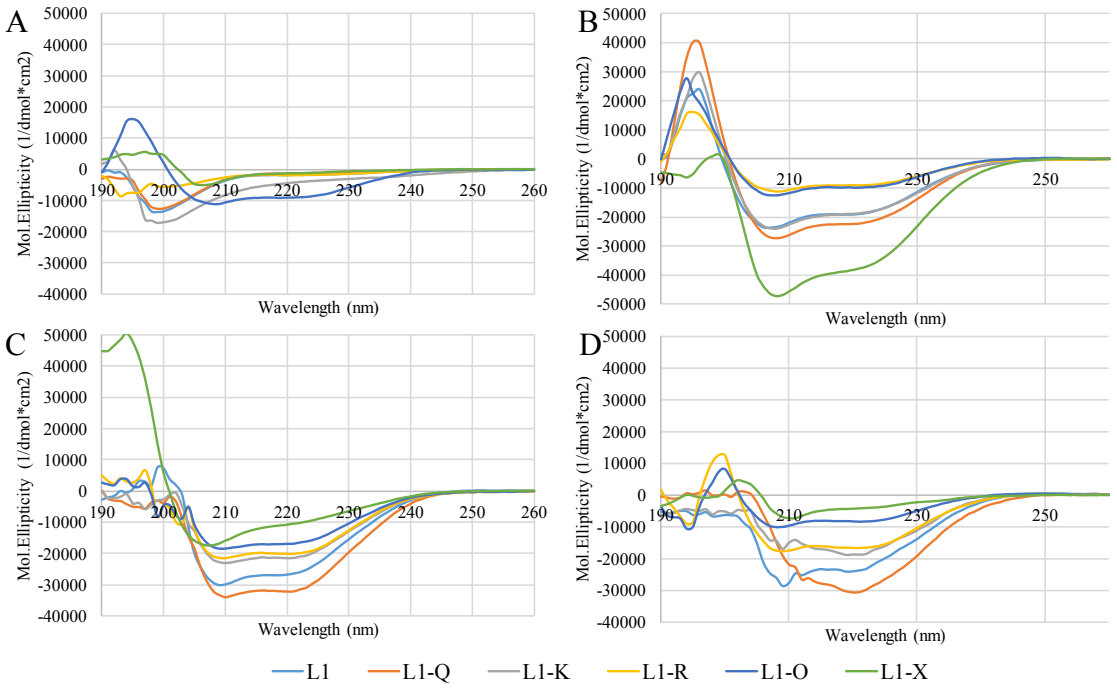

Figure 12. Circular Dichroism (CD) Spectroscopy. Spectra of all peptides were collected in, A, 10X diluted PBS, B, 50:50 PBS:TFE using the 10X diluted PBS, C, in the presence of 250 µM 3:1 PC:PG vesicles, or, D, in the presence of 250 µM 3:1 PC:Cholesterol vesicles. In 10X diluted PBS and 50:50 PBS:TFE, the peptide concentration was 5 µM, while in the presence of lipid vesicles, the peptide concentration was 3 µM. L1 is shown in light blue, L1-Q in orange, L1-K in gray, L1-R in yellow, L1-O in dark blue, and L1-X in green. All data represent the average of 64 scans with correction of background spectra lacking peptide.

Discussion

When analyzing the data, it is important to remember that the L1 peptide is derived from venom of an omnivorous species of ant which forages for both plants and insects as food [138]. Thus, the primary function of the venom peptides is not evolved for antimicrobial activity, but instead for offensive or defensive purposes. Additionally, venoms often contain multiple components which can act synergistically or act on

different and unrelated targets [139-141]. This can be further complicated by variations in the diet and habitat of the insect as well as the season [142].

Net charge. One of the goals of the current study was to investigate the role of net charge on AMP properties. Although the majority of AMPs that have been studied have a net positive charge, many, including L1, have anionic amino acids in the sequence. If net positive charge is a driving force for antimicrobial activity, evolutionarily there would be no selective pressure to retain these anionic amino acids in the sequence. However, this evolutionary pressure is not as clear in venom peptides, which can also act as antimicrobials.

In solution, the change of net charge from +5 to +6 or +7 did not have a significant impact on the REES results but were dramatically different for TCE quenching profiles. As the REES and TCE assays report on different aspects of Trp behavior (mobility and accessibility, respectively), the differences are potentially rooted in structural or aggregation state changes in the peptide in solution. [130-131, 143]

The CD spectra in Figure 11 indicate these three peptides (L1, L1-Q, L1-K) are not helical when in solution alone. However, the amino acid substitutions to change the net charge of the peptide are all at position 4, while the native Trp is at position 6 (Figure 1). These substitutions inherently likely do not impact the rotational freedom of the Trp, but may impact the local environment regarding polarity and/or the local packing of any aggregated form. Previous studies have shown that local interaction between anionic residues and Trp can impact spectral position and shifts [144-145], as well as peptide-peptide interactions [146-148].

The effect of increasing L1 net charge had marked effects on the antimicrobial efficacy against S. aureus and P. aeruginosa (Table 1). Increasing the charge from +5 to +6 resulted in an eightfold enhancement of activity against S. aureus and a twofold enhancement against P. aeruginosa while further increase of net charge to +7 further twofold increased the efficacy against P. aeruginosa. Notably, these changes also enhanced activity against E. coli and A. baumannii, but the parent L1 was already quite effective against those strains. This is consistent with previous reports that demonstrate cationic charge and net charge are important determinants of antimicrobial activity in AMPs [143, 149-151]. These changes, however, do not appear to be driven by increased ability to permeabilize vesicles or native membranes. While increasing the net charge did result in moderate enhancements to lipid binding, this enhancement was not dependent on bilayer charge. These results may point to a nonpermeabilizing role of L1 peptides in antimicrobial activity.

Additionally, altering the net charge on the peptide can alter the hydrophobic/hydrophilic balance of the sequence. Numerous studies on AMPs and peptidomimetic polymers have shown that this balance plays a key role in antimicrobial activity, cytotoxicity, and interactions with lipid bilayers [152-153]. In the peptides presented here, the overall hydrophobic balance is not significantly impacted as E to Q to K changes at position 4 are all polar. Notably, Gln is an uncharged polar residue which is naturally less polar than Lys, but does not result in major differences in lipid bilayer binding or antimicrobial activity. As such, any small changes in the hydrophobic/hydrophilic balance, if at all, are swamped by the change in net charge.

Cationic side chain identity. While the net charge of the peptide does appear to play some role in activity and may have strain-specific influences, previous studies on peptides and peptidomimetic polymers have shown that not all cationic groups behave identically in AMPs. Side chain length and cationic moiety identity have both been shown to dramatically impact characteristics of antimicrobials [154-157]. Additionally, the well-studied TAT sequence, originally derived from HIV, has shown a necessity for Arg residues to function in membrane translocation [158-159]. In the L1 background, switching Lys to Arg had minimal effects on MIC and MBC for all strains tested, except P. aeruginosa which had a marked decrease in efficacy. Interestingly, the Lys to Arg substitution resulted in a twofold decrease in MIC (increased efficacy) against E. coli, consistent with several Trp-rich sequences described by Arias et al. A number of studies have shown that Arg substitutions for Lys would enhance antimicrobial activity [160-161], likely from an increased H-bonding network and ability to interact with more lipid molecules for each cationic moiety [162].

Side chain length also clearly plays a role in activity and characteristics of the L1 peptides. Reducing the side chain length by one methyl group (Lys to Orn) had little effect on efficacy or binding, but reduction by three methyl groups (Lys to Dap) dramatically increased the MIC values. This is consistent with previous results on AMPs and peptidomimetic polymers. However, a recent report by Hodges and coworkers has shown the inclusion of Dap in AMPs can cause a small reduction of antibacterial activity but can have a significant reduction in hemolytic activity, improving the overall therapeutic potential [163]. The loss of activity from shortening the length of the cationic side chain has been attributed to peptide penetration depth in the bilayer, the Dap side

chain forcing a shallower, less disruptive conformation. The DQA results indicate that the L1-X does appear to adopt a shallower orientation in PE:PG membranes (model of bacterial membranes) but shows less of a difference compared to the L1-K in PC or PC:PG membranes. This is consistent with the best performing sequences against E. coli also exhibiting the greatest OM disruption and lowest Q-ratio in PE:PG membranes.

Chapter 3

Synergistic Interactions of Ionic Liquids and Antimicrobials to Improve Efficacy

Introduction

Physiochemical properties of ionic liquids. Ionic liquids (ILs) are classified as novel organic salts, that exist in liquid form at room temperature [164-165]. ILs are composed of large organic cations or anions with alkyl chain substituents that can alter the hydrophobicity of the molecule. Common cations found in ILs include imidazolium or pyridinium, while anions include hexafluorophosphate, tetrafluoroborate, chloride, nitrate, and bromide [166]. ILs have been studied for a variety of applications such as electrochemical, industrial, and biomedical. Although there are many studies focusing on electrochemical applications, potential applications include drug delivery, enzymatic reaction enhancement, and use as biomaterials. ILs are advantageous due to their unique physiochemical properties such as low melting points, exceptional solvation potential, low volatility, and negligible vapor pressure [82]. These properties are able to be manipulated easily by altering their ions, alkyl chain length, or type of head group [167-168]. Long-chain imidazolium based ILs exhibit an amphiphilic conformation with a charged hydrophilic head group and hydrophobic tail [169]. When in aqueous solution, ILs exhibit a rod-like micelle formation [170-171].

Ionic liquids as antimicrobials. Studies have shown prominent antibacterial activity of imidazolium ILs against bacteria and fungi due to their surfactant-like properties [172-173]. However, the antimicrobial activity of each IL is dependent on the length of the alkyl chain. A study performed by *Cook et al.,* had shown as the alkyl chain increased, so

did the antimicrobial activity. The imidazolium salts with 8 carbon atoms in the chain exhibited activity against a broad spectrum of both Gram-positive and Gram-negative bacteria. Their results concluded that antimicrobial activities correlate to ILs hydrophobicities (increasing alkyl chain length). However, while ILs have been shown to exhibit antimicrobial activity and the mechanism of action has begun to be explored, several key challenges must be overcome to identify whether ILs have potential as therapeutic agents.

A promising method for use of ILs as antimicrobials, is to enhance efficacy of existing antimicrobials in combination with ILs. This study combines imidazolium chloride based ILs with differing alkyl tails in combination with various commercially available antimicrobials to examine the potential synergistic antimicrobial effects on various bacteria, along with human cells to determine cytotoxic limits.

Materials and Methods

Ionic liquid preparation. Ionic liquids used in this study: 1-ethyl-3-methylimidazolium chloride, [EMIM]Cl, Sigma; 1-butyl-3-methylimidazolium chloride, [BMIM]Cl, Sigma; 1-hexyl-3-methylimidazolium chloride, [HMIM]Cl, Alfa Aesar; and 1-octyl-3-methylimidazolium chloride, [OMIM]Cl, Alfa Aesar; ([DMIM]Cl). Solutions of IL at indicated concentration created with either PBS (Phosphate Buffer System) or water solvent as indicated by experiment.

Critical micelle concentration (CMC) with tetracycline. Stocks of 2 mM sodium phosphate buffer, 10 ug/mL Tetracycline, and 1.0 M [OMI]Cl, and [DMI]Cl were prepared. DPH concentration was determined by absorbance spectroscopy using ε_{350} =

88,000 [174]. In a black, clear flat bottom 96-well plate, 50 µL of serially diluted IL was placed in each well. Then, calculated amount of buffer was added to each well. Once all wells contained buffer and IL, correct amount of tetracycline for final concentrations of 1 µg/mL, 0.1 µg/mL, 0.01 µg/mL, or 0 µg/mL was added to the wells. Right before measurement, DPH (final concentration 2.5µM) was added with gentle mixing by pipetting to ensure no bubbles were formed. Samples were measured using λex = 358 nm and λem = 430 nm.

Bacterial culturing. Bacteria were streaked on LB-Miller agar plates from a frozen glycerol stock (-80°C) (*Escherichia coli* D31 [124], *Staphylococcus aureus* ATCC 35556, *Pseudomonas aeruginosa* PA-01 [175], *Acinetobacter baumannii* ATCC 19606, *Klebsiella pneumoniae* ATCC 700603, *Bacillus subtilis* ATCC:6051). An overnight was prepared using a single colony of each bacterial strain into fresh LB broth and placed into a shaking incubator 37°C at 225 rpm for ~18 hours. After incubating overnight, a fresh 1:200 dilution was made in LB broth and used for the experiment.

Minimal Inhibitory Concentration (MIC). Same procedure performed as described in Chapter 2.

Results

Previous work has demonstrated antimicrobial effects of ILs and a strong correlation between increased alkyl-chain length and minimal inhibitory concentration (MIC) [91, 176]. In this study we evaluated both the magnitude of this antimicrobial effect as well the potential mechanism of actions for 3-methylimidazolium chloride ILs of differing in alkyl chain length (Figure 13).

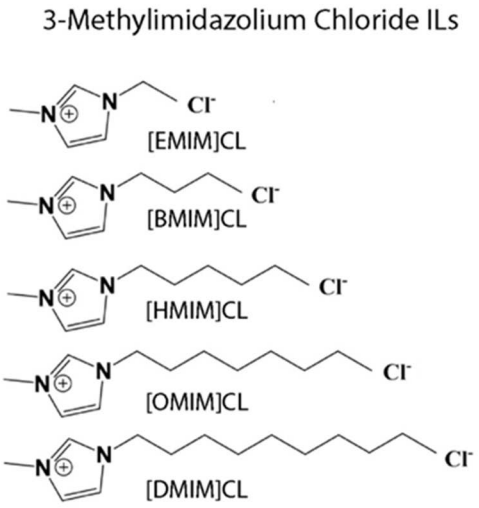

Figure 13. Imidazolium Chloride Ionic Liquids with Various Alkyl Chain Lengths

Critical Micelle Concentrations (CMCs) with tetracycline. A possible mechanism for antimicrobial effects of ILs include the ability of the IL to act as a detergent and destabilize the cell membrane. An alternative hypothesis is that the amphipathic nature of ILs may directly impact an associated antimicrobial compound through the formation of micelles. Micelles are roughly spherical structures formed by amphiphilic molecules in which the nonpolar portion of the molecule is buried at the interior of the structure while the polar portions are exposed, favorably interacting with the aqueous environment. Previous work has shown that some imidazolium ILs can form micelles and thus if antimicrobials affect the CMC, it would inherently impact the antimicrobial activity [177]. Using a fluorescence-based assay with the environmentally sensitive fluorophore DPH, CMC of [OMIM]Cl and [DMIM]Cl was measured in the absence or presence of various concentrations of tetracycline (Figure 14). In this assay, DPH fluorescence intensity increases dramatically upon formation of micelles due to DPH partitioning into the nonpolar core of the micelle [174]. The data shows that tetracycline has minimal

effect on the formation of micelles over a 100-fold concentration range tested compared to the no tetracycline control for both ILs examined. Thus, any effects of tetracycline in combination with ILs are likely due to true synergistic behavior rather than influence on micellar properties.

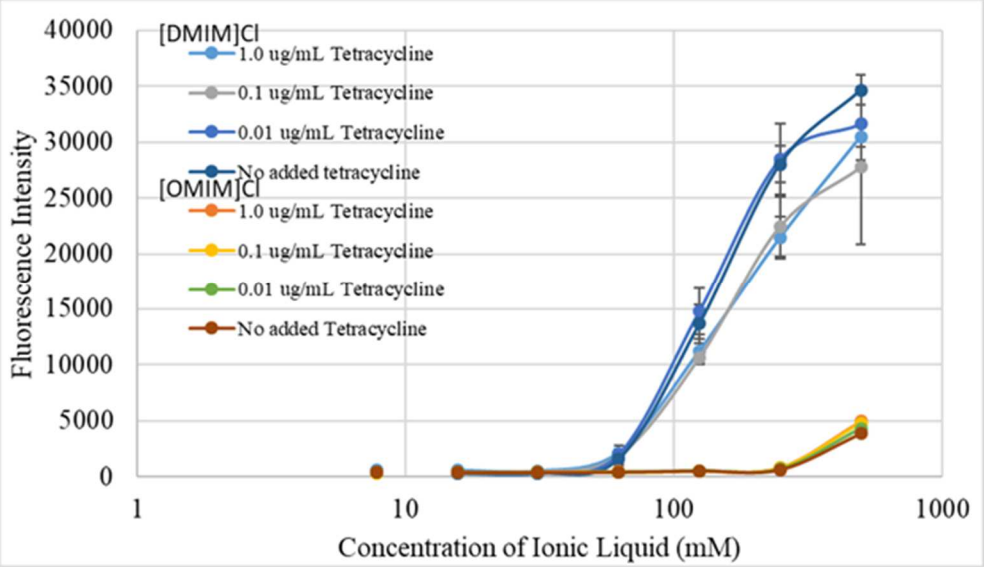

Figure 14. Critical Micelle Concentration (CMC) with Tetracycline. Imidazolium chloride ILs with various alkyl chain lengths tested in combination with tetracycline

Minimum Inhibitory Concentration (MIC). Microbial inhibition effects were evaluated using 3-methylimidazolium chloride ILs of differing in alkyl chain length with six microbial strains (*S. aureus, B. subtilis, P. aeruginosa*, *K. pneumoniae, E. coli*, *S. aureus,* and *A. baumanii*). In agreement with other studies, baseline MIC experiments suggest that alkyl chain lengths of 6, 8, and 10 exhibit independent antimicrobial effects with longer chain lengths exhibiting the greatest inhibition across a variety of

microorganisms (Table 4). MIC values, there is a direct correlation between longer alkyl chain lengths**.** For those ILs which presented with an antimicrobial effect, [HMIM]Cl, [OMIM]Cl, and [DMIM]Cl demonstrated a direct correlation between IL concentration, and ability to inhibit bacterial growth.

Table 4

MIC (mM) of ILs

	S. aureus	*B. subtilis*	*P. aeruginosa*	*K. pneumoniae*	*E. coli*	*A. baumannii*
[EMIM]Cl	>100	>100	>100	>100	>100	>100
[BMIM]Cl	100	>100	>100	>100	100	100
[HMIM]Cl	12.5	50	25	25	6.25	12.5
[OMIM]Cl	1.25	5	10	5	1.25	5
[DMIM]Cl	0.31	0.625	5	2.5	0.31	1.25

Note. MIC, Minimum Inhibitory Concentration

Discussion

Amphiphilic molecules, such as ILs, can act as antimicrobials by interacting with the bacterial membrane in a detergent like manner causing destabilization of the membrane [178]. The activity of these molecules is linked to the monomer-micelle equilibrium, which dramatically changes the physical and chemical properties of the molecules. Several lines of experiments point to the ability of imidazolium chloride-based ILs to permeabilize cell membranes. Previous work has shown that some of these

imidazolium ILs can form micelles and thus if tetracycline affects the CMC, it could inherently impact the antimicrobial activity [177]. Micelle formation is primarily governed by concentration, and the concentration at which micelles form is known as the Critical Micelle Concentration (CMC). CMC has been shown to be influenced by salt concentration and other additives in solution [179]. Our results point to the fact that tetracycline does not significantly affect the ability of [OMIM]Cl or [DMIM]Cl to form micelles (Figure 14). One possible interpretation of this finding is that tetracycline does not enhance the detergent-like properties of ILs action on the cellular membrane, but rather the addition of [OMIM]Cl or [DMIM]Cl to microbial populations acts independently of antimicrobial compound to elicit a membrane destabilizing effects to enhance the efficacy of the antimicrobial compound applied.

Other experiments were performed to determine synergistic effects of imidazolium chloride based ILs and broad spectrum of commercially available antibiotics, along with testing human cyctotoxicity (data not shown). These tests consisted of a permeability assay using flow cytometry, bactericidal disc assay (zone of inhibition assay), and treatment of HeLa cells in the presence of ILs and tetracycline. When combining imidazolium chloride based ILs with an alkyl chain of 6 and 8, synergistic interactions with a wide-range of antimicrobials was shown. Two separate complementary assays were performed, a 96-well liquid culture and a zone of inhibition (ZOI) disc assay. The results (data not shown) exhibited that when ILs ([HMIM]Cl and [OMIM]Cl) and commercial antimicrobials (tetracycline (12.5 mg/mL), doxycycline hyclate (10 mg/mL), and clindamycin (5 mg/mL)) were used in combination, the necessary concentration of antimicrobial compound to inhibit growth was reduced.

Interestingly, while a surprisingly large number of different antimicrobials were enhanced by the addition of IL, many trends point to specific modes of action for synergy of IL and antimicrobials. One of the strongest examples of synergism, that was evident in various assays, was shown with addition of IL and tetracycline. The efficacy of doxycycline was also strongly enhanced in the ZOI experiments along with the antimicrobial clindamycin. These three antibiotics are in the tetracycline family, an antibiotic class that inhibits protein synthesis by targeting the 30S ribosomal subunit [184]. It has been suggested that the limited efficacy of tetracycline, as well as the mechanism for antibiotic resistance, revolves around limited uptake and retention by bacterial strains [185]. Given the potential membrane destabilizing effect of long-alkyl chain ILs, it is reasonable to hypothesize that the addition of IL enhances the ability of this class of antibiotics to enter and maintain higher concentrations within the bacterial cell.

Although ILs are known as biocompatible, non-toxic, and a green alternative, this classification is only realistically applied in limited concentrations. Recent reports highlight the toxicity of this class of molecules [186]. To examine the imidazolium based chloride ILs of varying alkyl chain length potential toxicity to mammalian cells, a combinatorial treatment of ILs and tetracycline was applied to mammalian cells. Through a limited approximation, the HeLa human cell line assays are the first step in identifying the potential human response to the combinatorial treatment of ILs and antibiotics [187]. When exposing human cell lines to high concentrations of ILs, toxicity is exhibited. However, HeLa cells treated with longer alkyl chain lengths, [OMIM]Cl, are less viable than when treated with [HMIM]Cl at the same final concentration. The results indicated

that when combining [HMIM]Cl and tetracycline, a clear synergistic response was shown in the reduced amount of tetracycline required to reach 70% lethality in *P. aeruginosa*, and the addition of [HMIM]Cl to HeLa cells did not increase the toxicity of tetracycline in culture. This suggests that the combination of imidazolium chloride based ILs with antimicrobials is able to reduce the amount of antibiotic necessary to combat bacterial growth while having little to no additional toxic effect in human cell lines.

Chapter 4

Conclusions

Ponericin L1 Data

The data shows that the L1 peptide is a membrane-binding peptide that can adopt an α-helical conformation when bound to lipid bilayers. Both the net charge and the identity of the cationic groups on the peptide play a significant role in antimicrobial activity. As net charge increased from +5 to +7 the antimicrobial activity also increased. The shortened cationic side chains decreased the antimicrobial activity. Decreased antimicrobial activity in the shortened cationic side chains may be due to the peptide not being able to interact with the lipid bilayer as deeply as the longer side chains. The peptides adopted different conformations in zwitterionic and anionic vesicles which somewhat correlate to the antimicrobial activity. However, the *E. coli* OM disruption correlated best with MIC. The venom peptide L1 has good potential as a selective antimicrobial platform due to tunable activity and low hemolytic activity. Future studies on the hydrophobic/hydrophilic balance and the role of the polar face of the peptide should provide important fundamental understanding and will help in designing a more effective and selective antimicrobial molecule.

Antimicrobial Activity of Ionic Liquids Data

The data shows that there is an unknown synergistic interaction between imidazolium chloride based ILs and a broad class of antimicrobials against bacteria. Our results suggest that the combination of imidazolium chloride-based ILs with

antimicrobials is capable of reducing the amount of antibiotic necessary to combat bacterial growth while having little to no additional toxic effect in human cell lines. The mechanism of action for why the apparent enhancement of antibiotic delivery is effective in microbial cell populations but not mammalian cells is still unknown. One potential biochemical explanation is that antibiotic action is regulated by internal cellular concentration and that at typical treatment concentrations microbes have a baseline ability to exclude or remove antibiotics. Overall, the addition of ILs can enhance the delivery and/or retention of antimicrobials to both microbes and mammalian cells but due to the lack of specificity of antimicrobial targets in mammalian cells, the toxicity of the antimicrobial is not increased. Future investigations will need to be performed to assess the underlying mechanism that protects the mammalian cells from higher concentrations of antibiotics while simultaneously eliciting a synergistic response in improving the efficacy of antimicrobial compounds for combating bacterial growth.

References

[1] Mohr K.I. (2016). History of Antibiotics Research. In: Stadler M., Dersch P. (eds) How to Overcome the Antibiotic Crisis. *Current Topics in Microbiology and Immunology, vol 398.* Springer, Cham

[2] Noakes T.D., Borresen J., Hew-Butler T., Lambert M.I., Jordaan E. (2008). Semmelweis and the aetiology of puerperal sepsis 160 years on: an historical review. *Epidemiol Infect. 136(1)*, 1–9.

[3] Jenssen H, Hamill P, Hancock RE. (2006). Peptide antimicrobial agents. *Clin Microbiol Rev. 19*, 491–511.

[4] Bahar AA, Ren D. (2013). Antimicrobial peptides. *Pharmaceuticals (Basel) 6*, 1543–75.

[5] Clardy J., Fischbach M. A., & Currie C. R. (2009). The natural history of antibiotics. *Current biology, 19(11)*, R437-R441.

[6] Munita J. M., Arias C. A. (2016). Mechanisms of Antibiotic Resistance. *Microbiol Spectr 4(2).*

[7] Alós JI. (2015). Resistencia bacteriana a los antibióticos: una crisis global [Antibiotic resistance: A global crisis]. *Enferm Infecc Microbiol Clin. 33(10),* 692□699.

[8] Travis J. (1994). Reviving the antibiotic miracle? *Science 264*, 360–362.

[9] Prestinaci F., et al. (2015). Antimicrobial resistance: a global multifaceted phenomenon. *Pathog Glob Health 109(7)*, 309-318.

[10] Oyston, P.C., Fox, M.A., Richards, S.J., and Clark, G.C. (2009). Novel peptide therapeutics for treatment of infections. *J Med Microbiol 58*, 977–987.

[11] Marshall, S.H., and Arenas, G. (2003). Antimicrobial peptides: A natural alternative to chemical antibiotics and a potential for applied biotechnology. *Electron J Biotechn 6*, 271–284.

[12] Kosciuczuk EM, Lisowski P, Jarczak J, Strzalkowska N, Jozwik A, Horbanczuk J, Krzyżewski J, Zwierzchowski L, Bagnicka E. (2012). Cathelicidins: family of antimicrobial peptides. A review. *Mol Biol Rep. 39*, 10957–70.

[13] Starr CG, Maderdrut JL, He J, Coy DH, Wimley WC. (2018). Pituitary adenylate cyclase-activating polypeptide is a potent broad-spectrum antimicrobial peptide: structure-activity relationships. *Peptides. 104*, 35–40.

[14] Dubos R.J. (1939). Studies on a bactericidal agent extracted from a soil bacillus: II. Protective effect of the bactericidal agent against experimental Pneumococcus infections in mice. *J. Exp. Med. 70*, 11–17.

[15] Hotchkiss R.D., Dubos R.J. (1940). Fractionation of the bactericidal agent from cultures of a soil Bacillus. *J. Biol. Chem. 132*, 791–792.

[16] Van Epps H.L. (2006). Rene dubos: Unearthing antibiotics. *J. Exp. Med. 203*, 259.

[17] Dubos R.J., Hotchkiss R.D. (1941). The production of bactericidal substances by aerobic sporulating bacilli. *J. Exp. Med. 73*, 629–640.

[18] Rammelkamp C.H., Weinstein L. (1942). Toxic effects of tyrothricin, gramicidin and tyrocidine. *J. Infect. Dis. 71*, 166–173.

[19] Ohtani S., Okada T., Yoshizumi H., Kagamiyama H. (1977). Complete primary structures of two subunits of purothionin a, a lethal protein for brewer's yeast from wheat flour. *J. Biochem. 82*, 753–767.

[20] Hirsch J.G. (1956). Phagocytin: A bactericidal substance from polymorphonuclear leucocytes. *J. Exp. Med. 103,* 589–611.

[21] "User's Guide." LAMP2: An Update to LAMP Database Linking Antimicrobial Peptide., 2016, biotechlab.fudan.edu.cn/database/lamp/guide.php.

[22] Zhao X., Wu H., Lu H., Li G., Huang Q. (2013). Lamp: A database linking antimicrobial peptides. *PLoS One. 8*, e66557.

[23] Zasloff M. (2002). Antimicrobial peptides of multicellular organisms. *Nature. 415,* 389–395.

[24] Schauber J., Gallo R.L. (2008). Antimicrobial peptides and the skin immune defense system. *J. Allergy Clin. Immunol. 122*, 261–266.

[25] Ganz T. (2003). The role of antimicrobial peptides in innate immunity. *Integr. Comp. Biol. 43*, 300–304.

[26] Niyonsaba F., Iwabuchi K., Matsuda H., Ogawa H., Nagaoka I. (2002). Epithelial cell-derived human beta-defensin-2 acts as a chemotaxin for mast cells through a pertussis toxin-sensitive and phospholipase c-dependent pathway. *Int. Immunol. 14,* 421–426.

[27] Hancock R.E., Scott M.G. (2000). The role of antimicrobial peptides in animal defenses. *Proc. Natl. Acad. Sci. USA. 97*, 8856–8861.

[28] Oppenheim J.J., Biragyn A., Kwak L.W., Yang D. (2003). Roles of antimicrobial peptides such as defensins in innate and adaptive immunity. *Ann. Rheum. Dis. 62*, ii17–ii21.

[29] Radek K., Gallo R. (2007). Antimicrobial peptides: Natural effectors of the innate immune system. *Semin. Immunopathol. 29,* 27–43.

[30] Conlon J.M., Sonnevend A. (2010). Antimicrobial peptides in frog skin secretions. *Methods Mol. Biol. 618,* 3–14.

[31] Ma Y.F., Liu C.B., Liu X.H., Wu J., Yang H.L., Wang Y.P., Li J.X., Yu H.N., Lai R. (2010). Peptidomics and genomics analysis of novel antimicrobial peptides from the frog, *Rana nigrovittata*. *Genomics. 95,* 66–71.

[32] Zasloff, M. (1987). Magainins, a class of antimicrobial peptides from Xenopus skin: isolation, characterization of two active forms, and partial cDNA sequence of a precursor. *Proceedings of the National Academy of Sciences*.

[33] Schäfer-Korting, M., & Rolff, J. (2018). Skin delivery of antimicrobial peptides. *In Emerging Nanotechnologies in Immunology*, 23–45.

[34] Hollmann A, Martinez M, Maturana P,Semorile LC and Maffia PC. (2018). Antimicrobial Peptides: Interaction with model and biological membranes and synergism with chemical antibiotics. *Front. Chem. 6*, 204.

[35] Kuroda, K., Okumura, K., Isogai, H., & Isogai, E. (2015). The human cathelicidin antimicrobial peptide LL-37 and mimics are potential anticancer drugs. *Frontiers in oncology, 5*, 144.

[36] Robinson Jr, W. E., McDougall, B., Tran, D., & Selsted, M. E. (1998). Anti□HIV□1 activity of indolicidin, an antimicrobial peptide from neutrophils. *Journal of leukocyte biology, 63(1),* 94-100.

[37] Tsai, P. W., Yang, C. Y., Chang, H. T., & Lan, C. Y. (2011). Human antimicrobial peptide LL-37 inhibits adhesion of Candida albicans by interacting with yeast cell-wall carbohydrates. *PloS one, 6(3),* e17755.

[38] Ullal, A. J., & Noga, E. J. (2010). Antiparasitic activity of the antimicrobial peptide HbβP□1, a member of the β□haemoglobin peptide family. *Journal of fish diseases, 33(8),* 657-664.

[39] Loeffler J.M., Nelson D., Fischetti V.A. (2001). Rapid killing of Streptococcus pneumoniae with a bacteriophage cell wall hydrolase. *Science. 294*, 2170–2172.

[40] Hancock REW, Lehrer R. (1998). Cationic peptides: a new source of antibiotics. *Trends Biotechnol. 16*, 82–8.

[41] Epand, R. M., & Vogel, H. J. (1999). Diversity of antimicrobial peptides and their mechanisms of action. *Biochimica et Biophysica Acta (BBA)-Biomembranes, 1462(1-2)*, 11-28.

[42] Huang Y.B., Huang J.F., Chen Y.X. (2010). Alpha-helical cationic antimicrobial peptides: Relationships of structure and function. *Protein Cell. 1*, 143–152.

[43] Bulet P., Stocklin R., Menin L. (2004). Anti-microbial peptides: From invertebrates to vertebrates. *Immunol. Rev. 198*, 169–184.

[44] McManus A.M., Dawson N.F., Wade J.D., Carrington L.E., Winzor D.J., Craik D.J. (2000). Three-dimensional structure of rk-1: A novel alpha-defensin peptide. *Biochemistry. 39*, 15757–15764.

[45] Uteng M., Hauge H.H., Markwick P.R., Fimland G., Mantzilas D., Nissen-Meyer J., Muhle-Goll C. (2003). Three-dimensional structure in lipid micelles of the pediocin-like antimicrobial peptide sakacin p and a sakacin p variant that is structurally stabilized by an inserted c-terminal disulfide bridge. *Biochemistry. 42,* 11417–11426.

[46] Tossi A, Sandri L, Giangaspero A. (2000). Amphipathic, alpha-helical antimicrobial peptides. *Biopolymers. 55(1),* 4-30.

[47] Som A, Vemparala S, Ivanov I, Tew GN. (2008). Synthetic mimics of antimicrobial peptides. *Biopolymers. 90,* 83–93.

[48] Mahlapuu M, Hakansson J, Ringstad L, Bjorn C. (2016). Antimicrobial peptides: an emerging category of therapeutic agents. *Front Cell Infect Microbiol. 6,* 194.

[49] Hancock R. E., & Rozek A. (2002). Role of membranes in the activities ofantimicrobial cationic peptides. *FEMS Microbiol. Lett. 206*, 143–149.

[50] Wimley W. C. (2010). Describing the mechanism of antimicrobial peptide action with the interfacial activity model. *ACS chemical biology, 5(10),* 905–917.

[51] Jakel CE, Meschenmoser K, Kim Y, Weiher H, Schmidt-Wolf IG. (2012). Efficacy of a proapoptotic peptide towards cancer cells. *In Vivo. 26*, 419–26.

[52] Pouny Y., Rapaport D., Mor A., Nicolas P., Shai Y. (1992). Interaction of antimicrobial dermaseptin and its fluorescently labeled analogues with phospholipid membranes. *Biochemistry. 31*, 12416–12423.

[53] Bechinger B. (2005). Detergent-like properties of magainin antibiotic peptides: A 31p solid-state nmr spectroscopy study. *Biochim. Biophys. Acta. 1712*, 101–108.

[54] Gazit E, Miller IR, Biggin PC, Sansom MSP, Shai Y. (1996). Structure and orientation of the mammalian antibacterial peptide cecropin P1 within phospholipid membranes. *J Mol Biol. 258*, 860–870.

[55] Costa F., Carvalho I.F., Montelaro R.C., Gomes P., Martins M.C. (2011). Covalent immobilization of antimicrobial peptides (AMPs) onto biomaterial surfaces. *Acta Biomater. 7,* 1431–1440.

[56] Papo N., Oren Z., Pag U., Sahl H.G., Shai Y. (2002). The consequence of sequence alteration of an amphipathic alpha-helical antimicrobial peptide and its diastereomers. *J. Biol. Chem. 277*, 33913–33921

[57] Westerhoff H.V., Juretic D., Hendler R.W., Zasloff M. (1989). Magainins and the disruption of membrane-linked free-energy transduction. *Proc. Natl. Acad. Sci. USA. 86,* 6597–6601.

[58] Subbalakshmi C., Nagaraj R., Sitaram N. (1999). Biological activities of c-terminal 15-residue synthetic fragment of melittin: Design of an analog with improved antibacterial activity. *FEBS Lett. 448*, 62–66.

[59] Park, Y. et al. (2007). Structure-activity relationship of HP (2–20) analog peptide: Enhanced antimicrobial activity by N-terminal random coil region deletion. *Biopolymers.*

[60] Lee D.G., Kim H.N., Park Y.K., Kim H.K., Choi B.H., Choi C.H., Hahm K.S. (2002). Design of novel analogue peptides with potent antibiotic activity based on the antimicrobial peptide, hp (2–20), derived from n-terminus of Helicobacter pylori ribosomal protein L1. *Biochim. Biophys. Acta. 1598*, 185–194.

[61] Chen L., Harrison S.D. (2007). Cell-penetrating peptides in drug development: Enabling intracellular targets. *Biochem. Soc. Trans. 35*, 821–825.

[62] Fernandez-Vidal M., Jayasinghe S., Ladokhin A.S., White S.H. (2007). Folding amphipathic helices into membranes: Amphiphilicity trumps hydrophobicity. *J. Mol. Biol. 370,* 459–470.

[63] Gao, B., & Zhu, S. (2018). Mesobuthus venom-derived antimicrobial peptides possess intrinsic multifunctionality and differential potential as drugs. *Frontiers in microbiology, 9,* 320.

[64] Pennington MW, Czerwinski A, Norton RS. (2018). Peptide therapeutics from venom: Current status and potential. *Bioorg. Med. Chem. 26,* 2738-2758.

[65] Lewis, R. J., & Garcia, M. L. (2003). Therapeutic potential of venom peptides. *Nature reviews drug discovery, 2(10),* 790-802.

[66] de Lima, D. C., Alvarez Abreu, P., de Freitas, C. C., Santos, D. O., Borges, R. O., Dos Santos, T. C., Mendes Cabral, L., Rodrigues, C. R., & Castro, H. C. (2005). Snake Venom: Any Clue for Antibiotics and CAM. Evidence-based complementary and alternative medicine: *eCAM, 2(1),* 39–47.

[67] Milne, T. J., Abbenante, G., Tyndall, J. D., Halliday, J. & Lewis, R. J. (2003). Isolation and characterization of a cone snail protease with homology to CRISP proteins of the pathogenesis-related protein superfamily. *J. Biol. Chem. 278*, 31105–31110.

[68] Blanchfield, J. T. et al. (2003). Synthesis, structure elucidation, in vitro biological activity, toxicity and Caco-2 cell permeability of lipophilic analogues of α-conotoxin MII. *J. Med. Chem. 46,* 1266–1272

[69] Huttner, A., et al. (2019). Oral amoxicillin and amoxicillin-clavulanic acid: properties, indications and usage. *Clin Microbiol Infect*.

[70] Montelongo-Peralta, L.Z., et al. (2019). Antibacterial Activity of combinatorial treatments composed of transition-metal/antibiotics against Mycobacterium tuberculosis. *Sci Rep, 9(1),* 5471.

[71] Opalski, A.S., et al. (2020). Combinatorial Antimicrobial Susceptibility Testing Enabled by Non-Contact Printing. *Micromachines (Basel), 11(2).*

[72] Welton, T. (1999). Room-Temperature Ionic Liquids. Solvents for Synthesis and Catalysis. *Chem Rev, 99(8),* 2071-2084

[73] Yu, L., et al. (2013). Conductivity, Spectroscopic, and Computational Investigation of H3O+ Solvation in Ionic Liquid BMIBF4. *Journal of Physical Chemistry B 117(23),* 7057-7064.

[74] Saha, D. and Mukherjee A. (2018). Effect of water and ionic liquids on biomolecules. *Biophys Rev. 10(3),* 795-808.

[75] Fiebig, O.C., et al. (2014). Quantitative evaluation of myoglobin unfolding in the presence of guanidinium hydrochloride and ionic liquids in solution. *J Phys Chem B. 118(2),* 406-12.

[76] Egorova KS, Gordeev EG, Ananikov VP. (2017). Biological activity of ionic liquids and their application in pharmaceutics and medicine. *Chem Rev. 117*, 7132–7189.

[77] Ventura SPM, e Silva FA, Quental MV, Mondal D, Freire MG, Coutinho JAP. (2017). Ionic-liquid-mediated extraction and separation processes for bioactive compounds: past, present, and future trends. *Chem Rev. 117*, 6984–7052.

[78] Schroder, C. (2017). Proteins in Ionic Liquids: Current Status of Experiments and Simulations. *Top Curr Chem (Cham) 375(2)*, 25.

[79] Itoh, T. (2017). Ionic Liquids as Tool to Improve Enzymatic Organic Synthesis. *Chem Rev, 117(15),* 10567-10607.

[80] Jumbri, K., et al. (2014). An insight into structure and stability of DNA in ionic liquids from molecular dynamics simulation and experimental studies. *Phys Chem Chem Phys 16(27),* 14036-46.

[81] Hanna, S.L., et al. (2017). Synergistic effects of polymyxin and ionic liquids on lipid vesicle membrane stability and aggregation. *Biophysical Chemistry*.

[82] Pendleton J.N, and Gilmore B.F. (2015). The antimicrobial potential of ionic liquids: A source of chemical diversity for infection and biofilm control. *Int. J. Antimicrobial Agents, 46*, 131-139.

[83] Alves, F., et al. (2013). Synthesis, characterization, and liposome partition of a novel tetracycline derivaalvestive using the ionic liquids framework. *Journal of Pharmaceutical Sciences, 102(5),* 1504-1512.

[84] Zhang, Y., et al. (2009). Synthesis and biological applications of imidazolium-based polymerized ionic liquid as a gene delivery vector. *Chem Biol Drug Des. 74(3),* 282.

[85] Jing, B., et al. (2016). Interaction of Ionic Liquids with a Lipid Bilayer: A Biophysical Study of Ionic Liquid Cytotoxicity. *The Journal of Physical Chemistry B. 120(10),* 2781-2789.

[86] Yoo, B., et al. (2014). Amphiphilic interactions of ionic liquids with lipid biomembranes: a molecular simulation study. *Soft Matter, 10(43),* 8641-8651

[87] Yoo B, Zhu Y, and Maginn EJ. (2016). Molecular Mechanism of Ionic-Liquid-Induced Membrane Disruption: Morphological Changes to Bilayers, Multilayers, and Vesicles. *Langmuir, 32(21)*, 5403-5411.

[88] Benedetto, A., et al. (2014). Structure and stability of phospholipid bilayers hydrated by a room-temperature ionic liquid/water solution: a neutron reflectometry study. *J Phys Chem B. 118(42),* 12192-206.

[89] Lim, G.S., Jaenicke S., and Klahn M. (2015). How the spontaneous insertion of amphiphilic imidazolium-based cations changes biological membranes: a molecular simulation study. *Phys Chem Chem Phys. 17(43),* 29171-83.

[90] Cole, M.R. (2012). Chemical and Biological Evaluation of Antibiotic-Based Ionic Liquids and Gumbos Against Pathogenic Bacteria. *LSU Doctoral Dissertations. 487.*

[91] Cook, K., et al. (2019). Correlating lipid membrane permeabilities of imidazolium ionic liquids with their cytotoxicities on yeast, bacterial, and mammalian cells. *Biomolecules, 9(6).*

[92] Raucci, M.G., et al. (2018). Antimicrobial Imidazolium Ionic Liquids for the Development of Minimal Invasive Calcium Phosphate-Based Bionanocomposites. *ACS Appl Mater Interfaces. 10(49),* 42766-42776.

[93] Jungnickel, C., et al. (2008). Micelle formation of imidazolium ionic liquids in aqueous solution. Colloids and Surfaces A: *Physicochemical and Engineering Aspects. 316(1)*. 278-284.

[94] Makarova O., Johnston P., Rodriguez-Rojas A., El Shazely B., Morales J.M., Rolff J. (2018). Genomics of experimental adaptation of Staphylococcus aureus to a natural combination of insect antimicrobial peptides. *Sci. Rep. 8,* 15359.

[95] Rozgonyi F., Szabo D., Kocsis B., Ostorházi E., Abbadessa G., Cassone M., Wade J.D., Otvos L., Jr. (2009). The antibacterial effect of a proline-rich antibacterial peptide A3-APO. *Curr. Med. Chem. 16*, 3996–4002.

[96] Jozefiak A., Engberg R.M. (2017). Insect proteins as a potential source of antimicrobial peptides in livestock production. A review. *J. Anim*. *Feed Sci. 26*, 87–99.

[97] Zhang L.J., Gallo R.L (2016). Antimicrobial peptides. *Curr. Biol. 26*, 14–19.

[98] Mylonakis E., Podsiadlowski L., Muhammed M., Vilcinskas A. (2016). Diversity, evolution and medical applications of insect antimicrobial peptides. *Philos. Trans. R. Soc. Lond. B. 371*.

[99] Orivel J., Redeker V., Le Caer J.P., Krier F., Revol-Junelles A.M., Longeon A., Chaffotte A., Dejean A., Rossier J. (2001). Ponericins, new antibacterial and insecticidal peptides from the venom of the ant Pachycondyla goeldii. *J. Biol. Chem. 276,* 17823–17829.

[100] Johnson S.R., Copello J.A., Evans M.S., Suarez A.V. (2010). A biochemical characterization of the major peptides from the Venom of the giant Neotropical hunting ant *Dinoponera australis*. *Toxicon. 55,* 702–710.

[101] Boman, H. G., and Hultmark, D. (1987). Cell-free immunity in insects. *Annu. Rev. Microbiol. 41*, 103–126

[102] Ekengren, S., and Hultmark, D. (1999). Drosophila cecropin as an antifungal agent. *Insect. Biochem. Mol. Biol.29*, 965–972

[103] Garcia F, Villegas E, Espino-Solis GP, Rodriguez A, PaniaguaSolis JF, Sandoval-Lopez G, Possani LD, Corzo G. (2013). Antimicrobial peptides from arachnid venoms and their microbicidal activity in the presence of commercial antibiotics. *Antibiot., 66*, 3

[104] Nolasco M, Biondi I, Pimenta DC, Branco A. (2018). Extraction and preliminary chemical characterization of the venom of the spider wasp *Pepsis decorate* (Hymenoptera: Pompilidae). *Toxicon, 150,* 74.

[105] Rodriguez, E. Villegas, A. Montoya-Rosales, B. Rivas-Santiago, G. Corzo. (2014). Characterization of antibacterial and hemolytic activity of synthetic pandinin 2 variants and their inhibition against *Mycobacterium tuberculosis. PLoS One, 9,* e101742

[106] Shukla, A., K. E. Fleming KE.,, H. F. Chuang HF., T. M. Chau TM., C. R. Loose CR., Stephanopoulos GN.G. N. Stephanopoulos, P. T. Hammond PT. (2010). Controlling the release of peptide antimicrobial agents from surfaces. *Biomaterials, 31*, 2348.

[107] H. Zhang H., J. Jiao J.,, H. Jin H. (2019). Degradable poly-L-lysine-modified PLGA cell microcarriers with excellent antibacterial and osteogenic activity. *Artificial Cells, Nanomedicine, and. Biotechnology. 2019, 47*, 2391.

[108] Y. Zhang Y., L. Zhang L., B. Li B., Y. Han Y. (2017). Enhancement in sustained release of antimicrobial peptide from dual-diameter-structured TiO2 nanotubes for long-lasting antibacterial activity and cytocompability. *ACS Appl. Mater. Interfaces 2017, 9,* 9449.

[109] Graham C., S. C. Richter SC., S. McClean S., E. O'Kane E., P. R. Flatt PR., C. Shaw C., (2006). Histamine-releasing and antimicrobial peptides from the skin secretions of the Dusky Gopher frog, *Rana sevosa*. *Peptides 2006, 27,* 1313-1319.

[110] Kozic, M., Fox, S. J., Thomas, J. M., Verma, C. S., & Rigden, D. J. (2018). Large scale ab initio modeling of structurally uncharacterized antimicrobial peptides reveals known and novel folds. *Proteins: Structure, Function, and Bioinformatics, 86(5),* 548-565.

[111] Pluzhnikov, K. A., Kozlov, S. A., Vassilevski, A. A., Vorontsova, O. V., Feofanov, A. V., & Grishin, E. V. (2014). Linear antimicrobial peptides from *Ectatomma quadridens* ant venom. *Biochimie, 107 Pt B,* 211–215.

[112] Simmaco, M., Mignogna, G., & Barra, D. (1998). Antimicrobial peptides from amphibian skin: what do they tell us? *Biopolymers, 47(6),* 435–450.

[113] Mor, A., and Nicolas, P. (1994). Isolation and structure of novel defensive peptides from frog skin. *European Journal of Biochemistry, 219(1□2),* 145-154.

[114] Amiche, M., Seon, A. A., Pierre, T. N., and Nicolas, P. (1999). The dermaseptin precursors: a protein family with a common preproregion and a variable C-terminal antimicrobial domain. *FEBS Lett. 456*, 352–356

[115] Kohn, E. M., Shirley, D. J., Arotsky, L., Picciano, A. M., Ridgway, Z., Urban, M. W., Carone, B. R., & Caputo, G. A. (2018). Role of Cationic Side Chains in the Antimicrobial Activity of C18G. *Molecules (Basel, Switzerland), 23(2),* 329

[116] Dathe, M.; Schumann, M.; Wieprecht, T.; Winkler, A.; Beyermann, M.; Krause, E.; Matsuzaki, K.; Murase, O.; Bienert, M. (1996). Peptide helicity and membrane surface charge modulate the balance of electrostatic and hydrophobic interactions with lipid bilayers and biological membranes. *Biochemistry 35,* 12612–12622.

[117] Tachi, T.; Epand, R.F.; Epand, R.M.; Matsuzaki, K. (2002). Position-dependent hydrophobicity of the antimicrobial magainin peptide affects the mode of peptide−lipid interactions and selective toxicity. *Biochemistry 41*, 10723–10731.

[118] Hicks, R.P, Bhonsle, J.B, Venugopal, D, Koser, B.W, Magill, A.J. (2007). De novo design of selective antibiotic peptides by incorporation of unnatural amino acids. *J. Med. Chem, 50,* 3026–3036

[119] Chen, Y.; Guarnieri, M.T.; Vasil, A.I.; Vasil, M.L.; Mant, C.T.; Hodges, R.S. (2007). Role of peptide hydrophobicityin the mechanism of action of alpha-helical antimicrobial peptides. *Antimicrob. Agents Chemother, 51,*1398–1406

[120] Hawrani, A.; Howe, R.A.; Walsh, T.R.; Dempsey, C.E. (2008). Origin of low mammalian cell toxicity in a class of highly active antimicrobial amphipathic helical peptides. J. Biol. Chem.2008,283, 18636–18645.

[121] Snider, C., Jayasinghe, S., Hristova, K., & White, S. H. (2009). MPEx: a tool for exploring membrane proteins. Protein science: a publication of the Protein Society, 18(12), 2624–2628.

[122] Shirley, D. J., Chrom, C. L., Richards, E. A., Carone, B. R., & Caputo, G. A. (2018). Antimicrobial activity of a porphyrin binding peptide. Peptide science (Hoboken, N.J.), 110(4), e24074.

[123] Caputo, G. A., & London, E. (2019). Analyzing Transmembrane Protein and Hydrophobic Helix Topography by Dual Fluorescence Quenching. In Lipid-Protein Interactions. *Methods Mol. Biol. 2003,* 351-368.

[124] Burman, L. G., Nordström, K., & Boman, H. G. (1968). Resistance of Escherichia coli to penicillins. V. Physiological comparison of two isogenic strains, one with chromosomally and one with episomally mediated ampicillin resistance. *Journal of bacteriology, 96(2),* 438–446.

[125] Capilato, J. N., Philippi, S. V., Reardon, T., McConnell, A., Oliver, D. C., Warren, A., Adams, J. S., Wu, C., & Perez, L. J. (2017). Development of a novel series of non-natural triaryl agonists and antagonists of the Pseudomonas aeruginosa LasR quorum sensing receptor. *Bioorganic & medicinal chemistry, 25(1),* 153–165.

[126] Caputo, G. A., & London, E. (2003). Cumulative effects of amino acid substitutions and hydrophobic mismatch upon the transmembrane stability and conformation of hydrophobic alpha-helices. *Biochemistry, 42(11),* 3275–3285.

[127] Chrom, C. L., Renn, L. M., & Caputo, G. A. (2019). Characterization and Antimicrobial Activity of Amphiphilic Peptide AP3 and Derivative Sequences. Antibiotics (Basel, Switzerland), 8(1), 20C.

[128] Wu, Y., Han, M. F., Liu, C., Liu, T. Y., Feng, Y. F., Zou, Y., et al. (2017a). Design, synthesis, and antiproliferative activities of stapled melittin peptides. *RSC Adv. 7,* 17514–17518Y.

[129] Zelezetsky, I., & Tossi, A. (2006). Alpha-helical antimicrobial peptides--using a sequence template to guide structure-activity relationship studies. *Biochimica et biophysica acta, 1758(9),* 1436–1449

[130] Raghuraman, H. and Chattopadhyay, A. (2006), Effect of ionic strength on folding and aggregation of the hemolytic peptide melittin in solution. *Biopolymers, 83:* 111-121.

[131] Haldar, S. Raghuraman, H. S. Haldar, H. Raghuraman, A. Chattopadhyay A. (2008), Monitoring orientation and dynamics of membrane-bound melittin utilizing dansyl fluorescence. *The Journal of Physical Chemistry B, 112 (44),* 14075-14082

[132] Nanda V, Cristian L, Toptygin D, Brand L, Degrado WF. (2013). Nanosecond Dynamics of InfluenzaA/M2TM and an Amantadine Resistant Mutant Probed by Time-Dependent Red Shifts of a Native Tryptophan. *Chemical physics. 2013*; 422.

[133] IUPAC. Compendium of Chemical Terminology, 2nd ed. (the "Gold Book"). Compiled by A. D. McNaught and A. Wilkinson. (1997). Blackwell Scientific Publications, Oxford (1997). Online version (2019-) created by S. J. Chalk. ISBN 0-9678550-9-8.

[134] Bolen, E. J., and Holloway, P. W. (1990) Quenching of tryptophan fluorescence by brominated phospholipid. *Biochemistry 29,* 9638−9643.

[135] Eftink, M. R., and Ghiron, C. A. (1976) Exposure of tryptophanyl residues in proteins. *Biochemistry 15,* 672−680.

[136] Ren, J., Lew, S., Wang, Z., and London, E. (1997) Biochemistry 36, 10213−10220

[137] Kachel, K., Asuncion-Punzalan, E., and London, E. (1995) Biochemistry 34, 15475−15479

[138] C. A. Schmidt, S. O. Shattuck, Zootaxa 2014, 3817, 1.

[139] D. O. Ceolin Mariano, U. C. de Oliveira, A. J. Zaharenko, D. C. Pimenta, G. Radis-Baptista, A. R. B. Prieto-da-Silva, Toxins 2019, 11, 448.

[140] G. Amorim, H. T. Longhim, C. T. Cologna, M. Degueldre, E. Pauw, L. Quinton, E. C. Arantes, J. Venom. Anim. Toxins Incl. Trop. Dis. 2019, 25, e148218.

[141] P. P. Santos, P. D. Games, D. O. Azevedo, E. Barros, L. L. de Oliveira, H. J. de Oliveira Ramos, M. C. Baracat-Pereira, J. E. Serrao, Arch. Insect Biochem. Physiol. 2017, 96, e21424

[142] C. T. Cologna, R. S. Rodrigues, J. Santos, E. de Pauw, E. C. Arantes, L. Quinton, J. Venom. Anim. Toxins Incl. Trop. Dis. 2018, 24, 6

[143] M. A. Hitchner, L. E. Santiago-Ortiz, M. R. Necelis, D. J. Shirley, T. J. Palmer, K. E. Tarnawsky, T. D. Vaden, G. A. Caputo, Biochim. Biophys. Acta Biomembr. 2019, 1861, 182984.

[144] Caputo GA, London E. (2004). *Biochemistry 43,* 8794.

[145] D. Jones, L. M. Gierasch, Biophys. J. 1994, 67, 1534.

[146] S. Lew, G. A. Caputo, E. London, Biochemistry 2003, 42, 10833.

[147] Rajagopal, M. S. Lamm, L. A. Haines-Butterick, D. J. Pochan, J. P. Schneider, Biomacromolecules 2009, 10, 2619

[148] Y. Wang, N. L. Truex, N. D. P. Vo, J. S. Nowick, Bioorg. Med. Chem. 2018, 26, 1151.

[149] Kuroda, G. A. Caputo, W. F. DeGrado, Chemistry 2009, 15, 1123

[150] Z. Jiang, A. I. Vasil, J. D. Hale, R. E. Hancock, M. L. Vasil, R. S. Hodges, Biopolymers 2008, 90, 369.

[151] Y. Rosenfeld, N. Lev, Y. Shai, Biochemistry 2010, 49, 853.

[152] D. Saint Jean, K. D. Henderson, C. L. Chrom, L. E. Abiuso, L. M. Renn, G. A. Caputo, Probiotics Antimicro. Proteins 2018, 10, 408.

[153] C. W. Avery, E. F. Palermo, A. McLaughlin, K. Kuroda, Z. Chen, Anal. Chem. 2011, 83, 1342.

[154] Arias, K. B. Piga, M. E. Hyndman, H. J. Vogel, Biomolecules 2018, 8, pii: E19.

[155] E. F. Palermo, K. Kuroda, Biomacromolecules 2009, 10, 1416

[156] E. F. Palermo, K. Kuroda, Appl. Microbiol. Biotechnol. 2010, 87, 1605

[157] S. Choi, A. Isaacs, D. Clements, D. Liu, H. Kim, R. W. Scott, J. D. Winkler, W. F. DeGrado, Proc. Natl. Acad. Sci. U. S. A. 2009, 106, 6968

[158] P. Richard, K. Melikov, E. Vives, C. Ramos, B. Verbeure, M. J. Gait, L. V. Chernomordik, B. Lebleu, J. Biol. Chem. 2003, 278, 585.

[159] S. Futaki, T. Suzuki, W. Ohashi, T. Yagami, S. Tanaka, K. Ueda, Y. Sugiura, J. Biol. Chem. 2001, 276, 5836.

[160] T. Nguyen, L. de Boer, S. A. Zaat, H. J. Vogel, Biochim. Biophys. Acta 2011, 1808, 2297.

[161] W. Schmidt, G. C. Wong, Curr. Opin. Solid State Mater. Sci. 2013, 17, 151.

[162] Li L, Vorobyov I, Allen TW. (2013). *Phys. Chem. B, 117*, 11906.

[163] Mant CT, Jiang Z, Gera L, Davis T, Nelson KL, Bevers S, Hodges RS. (2019). *Med. Chem. 62,* 3354.

[164] Welton, T. (1999). Room-Temperature Ionic Liquids. Solvents for Synthesis and Catalysis. *Chem Rev, 99(8),* 2071-2084.

[165] Yu, L., et al. (2013). Conductivity, Spectroscopic, and Computational Investigation of H3O+ Solvation in Ionic Liquid BMIBF4. *Journal of Physical Chemistry B, 117(23),* 7057-7064.

[166] Docherty KM, Kulpa Jr. CF. (2005). Toxicity and antimicrobial activity of imidazolium and pyridinium ionic liquids. *Green Chem. 7,* 185-189.

[167] Earle Martyn J, Seddon Kenneth R. (2000). Ionic liquids. Green solvents for the future. *Pure Appl Chem. 72*, 1391.

[168] Wasserscheid P, Keim W. (2000). Ionic liquids—new "solutions" for transition metal catalysis. *Angew Chem Int Ed. 39,* 3772–3789.

[169] Cornellas, A. et al. (2011). Self-aggregation and antimicrobial activity of imidazolium and pyridinium based ionic liquids in aqueous solution. Journal of colloid and interface science. *Journal of Colloid and Interface Science*.

[170] Liu X, Zhou G, He H, Zhang X, Wang J, Zhang S. (2015). Rodlike micelle structure and formation of ionic liquid in aqueous solution by molecular simulation. *Ind Eng Chem Res. 54,* 1681–1688.

[171] Vicent-Luna JM, Romero-Enrique JM, Calero S, and Anta JA. (2017). Micelle formation in aqueous solutions of room temperature ionic liquids: A molecular dynamics study. *The Journal of Physical Chemistry, 121 (35).*

[172] Kopecky F. (1996). *Pharmazie 51*, 135.

[173] Demberelnyamba D, Kim KS, Choi S.J, Park S.Y, Lee H, Kim CJ, Yoo I.D. (2004). *Bioorganic Med. Chem. 12*, 853.

[174] Chattopadhyay, A. and E. London. (1984). Fluorimetric determination of critical micelle concentration avoiding interference from detergent charge. *Anal Biochem, 139(2),* 408-12.

[175] Capilato, J.N., et al. (2017). Development of a novel series of non-natural triaryl agonists and antagonists of the Pseudomonas aeruginosa LasR quorum sensing receptor. *Bioorg Med Chem, 25(1),* 153-165.

[176] Ghanem, O.B., et al. (2015). Effect of imidazolium-based ionic liquids on bacterial growth inhibition investigated via experimental and QSAR modelling studies. *J Hazard Mater, 297*, 198-206.

[177] Lee, J.Y., et al. (2019). Effects of Ionic Liquid Alkyl Chain Length on Denaturation of Myoglobin by Anionic, Cationic, and Zwitterionic Detergents. *Biomolecules, 9(7).*

[178] Laatiris, A., et al. (2008). Antibacterial activity, structure and CMC relationships of alkanediyl alpha,omega-bis(dimethylammonium bromide) surfactants. *Microbiol Res, 163(6)*, 645-50.

[179] Palladino, P. and R. Ragone. (2011). Ionic strength effects on the critical micellar concentration of ionic and nonionic surfactants: the binding model. *Langmuir, 27(23)*. 14065-14070.

[180] Machado, L. R. & Ottolini, B. (2015). An Evolutionary History of Defensins: A Role for Copy Number Variation in Maximizing Host Innate and Adaptive Immune Responses. *Frontiers in immunology*.

[181] Hancock R.E. (1997). Peptide antibiotics. *Lancet (London, England)*, *349* (9049), 418–422.

[182] Dathe, M., Nikolenko, H., Meyer, J., Beyermann, M., & Bienert, M. (2001). Optimization of the antimicrobial activity of magainin peptides by modification of charge. *FEBS letters*, *501*(2-3), 146–150.

[183] Chang, T.-W. et al. (2017). Hydrophobic residues are critical for the helix-forming, hemolytic and bactericidal activities of amphipathic antimicrobial peptide TP4. *Plos One.*

[184] Connell, S.R., et al. (2003). Ribosomal protection proteins and their mechanism of tetracycline resistance. *Antimicrobial Agents and Chemotherapy. **47**(12),* 3675-3681.

[185] Reynard, A.M., Nellis L.F., and Beck M.E. (1971). Uptake of 3H-Tetracycline by resistant and sensitive *Escherichia coli*. *Appl Microbiol. 21(1),* 71-5.

[186] Pham, T.P., Cho C.W., and Yun Y.S. (2010). Environmental fate and toxicity of ionic liquids: a review. *Water Res, 44(2),* 352-72.

[187] Stepnowski, P., et al. (2004). Evaluating the cytotoxicity of ionic liquids using human cell line HeLa. *Hum Exp Toxicol, 23(11*), 513-7.